DEVELOPMENT OF AN X-BAND 25 WATT TRAVELING-WAVE TUBE

By

L. A. Roberts
and
R. I. Knight

17 March 1972

Contract No. 952931

This work was performed for the Jet Propulsion Laboratory, California Institute of Technology, sponsored by the National Aeronautics and Space Administration under Contract NAS7-100.

Final Report

Watkins-Johnson Company
3333 Hillview Avenue
Palo Alto, California

ABSTRACT

This is the final report on a program to develop a 25 watt high efficiency traveling-wave tube at 8.5 GHz for space communications and telemetry applications.

The report describes the design basis for the tube, which is known as the WJ-3703. Because of the combined high efficiency and high frequency requirements, the helix and body dimensions are very small and required the development of special techniques for various assembly and construction procedures. These are described in detail.

Measurement results of focusing tests and rf operation are given. Due to funding limitations coupled with design difficulties, only pulsed RF performance of the tubes was obtained. Tube performance is analyzed and recommendations for further development work are made.

I. INTRODUCTION

Purpose of Development Program

The main purpose of this program is to develop a high efficiency X-band traveling-wave tube. System requirements are shifting from S to X band because higher data rates are obtainable at the higher frequency for a given power level. Projected power level requirements lie within the 20 to 50 watt power range.

These requirements have been projected primarily for deep space missions where power budgets are severely limited. Because of the low sunlight intensity in the outer planet region, Radioisotope Thermoelectric Generator (RGT) power sources are to replace the solar panel arrays. This makes efficient conversion of dc to RF energy extremely important and requires the development of a highly efficient traveling-wave tube.

Basis of Design

The use of the traveling-wave tube as a spacecraft power amplifier is well established because of its demonstrated long life and high efficiency capabilities. It also has demonstrated the ability to meet environmental requirements associated with space craft launch, re-entry and landing, high vacuum space operation and normal operation after sterilization.

High efficiency designs (45 to 50 percent overall efficiency) have already been developed at S-band (2300 MHz). Efficiency is achieved in these designs by a combination of high basic beam conversion efficiency (36 to 37 percent of dc input power converted to rf power output), recovery of some of the unconverted beam energy using depressed collector techniques (an additional 10 to 12 percentage points) and low power heater-cathode designs. Overall efficiency of S-band space TWT's in the 25 to 100 watt power range has been demonstrated to be in the range of 45 to 50 percent. Generally the higher efficiency occurs at the higher power level.

Scaling of these designs to X-band can be done while maintaining high overall efficiency performance. This is achieved with large over-voltage operation to obtain the highest possible beam efficiency and depressed collector techniques to obtain further efficiency improvement. The shift to the higher frequency of X-band causes a major size reduction in both the TWT helix diameter and the electron beam diameter.

All of the normalized design parameter values cannot be maintained in the frequency scaling for reasons discussed later. As a result, a lower beam efficiency is obtained and more efficiency improvement must be achieved with depressed collector techniques.

Specific Areas of Development Needed for Shift from S-band to X-band.

Thermal Transfer

When the size of the helix is reduced while maintaining the RF power output level at 50 watts, the thermal power density flowing in the helix structure is increased. Heat is generated in the helix due to both rf losses and helix current interception. This must be conducted out through the metal helix tape, the ceramic helix support rods, the metal vacuum envelope, the magnet structure and the capsule to the external heat sink. Thus, close attention must be paid to the thermal design. The major change in the helix itself was to work out techniques of providing short heat paths in the helix and more heat paths to the external body structure. This was accomplished by incorporating more ceramic support rods in the helix structure.

Helix and Vacuum Envelope Construction

In scaling from S-band to X-band it is necessary to make a diameter reduction of the helix by a factor of 3.0:1. Techniques of construction and assembly of the helix at the lower frequencies were found to be inadequate for the smaller structure at the higher frequencies. A number of different approaches had to be worked out to accomplish the precision assembly necessary for the helix and body.

Two-Stage Depressed Collector

Because of the lower beam efficiency which is a result of the higher frequency design, a larger efficiency improvement factor is necessary from the depressed collector operation. The collector design must be modified from the single-stage design used at S-band to a two-stage design. This is to allow a more optimum velocity sorting of the electrons which exit from the helix. This will lead to greater efficiency improvement factors.

Use of High-Energy-Product Magnet Materials

The higher current density electron beam which results from the smaller beam diameter requires higher peak magnetic fields in the focusing system to confine the beam. This plus other factors having to do with the period of the

periodic permanent magnet (PPM) focusing system dictates the use of high-coercive-force materials as magnets, such as platinum-cobalt and samarium-cobalt. Samarium-cobalt is a relatively new material and has a coercive force nearly twice that of platinum-cobalt. It has presented problems in magnetization and demagnetization because of its high coercive force and straight line demagnetization curve. It will be used in the most critical region of the magnet structure to achieve the necessary high peak fields. Existing magnet treating equipment was inadequate to adequately magnetize and demagnetize the material. New coils were obtained and a series of trials and redesigns were necessary before satisfactory performance could be obtained.

II. GENERAL SUMMARY

Objectives

The detailed objectives of this program are given in the Jet Propulsion Laboratory Specification CS505093B. These specifications were the basis of approximately the first three months of the program effort. At that point in time, because of NASA budget cutbacks, JPL had to reduce the total program cost budget to 54 percent of the negotiated contract cost level. Because of this cost limitation, the program goals had to be modified to reflect what were felt to be reasonable objectives for a reduced program. The area which appeared to be most easily eliminated without damaging ultimate system requirements was the high power mode of operation. Thus, the interim program goals were shifted to a single mode requirement at a 25 watt power output level. The overall efficiency goals for this power level remained at 42 percent. It was deemed desirable, however, to try to maintain the tube construction to allow an easy shift back to the 50 watt/25 watt dual mode capability if future systems required it. The revised design goals are shown in Table I.

Design Approach

Large Overvoltage Design

Experience with high efficiency tubes at S-band has shown that the overall efficiency of a TWT is highest when the beam efficiency is the highest. The highest beam efficiency is obtained with a design technique known as large overvoltage design.[1,2] With this design technique, the highest efficiency is obtained at the highest value of beam perveance which can be focused satisfactorily. The defocusing effects which ultimately limit the perveance are the helix current interception under large signal saturated power output conditions. Because of the decrease in the helix and beam size in shifting the tube design to X-band from S-band, the value of beam perveance which can be focused decreases. As a consequence, the maximum beam efficiency which can be obtained also decreases. To meet the high overall efficiency requirements which are imposed, greater efficiency improvement must be obtained from the depressed collector operation. This will be accomplished with a two-stage collector as described later.

TABLE I

REVISED DESIGN GOALS

Frequency Band	8400 - 8500 MHz
Nominal	8415 MHz
Power Output	25 W
Gain	37 dB minimum
Bandwidth (1 dB Points)	30 MHz
Overall Efficiency	42 Percent
Input Match (Hot) VSWR	1.5:1 maximum
Output Load (Stable Operation) VSWR	1.75:1
Harmonics	10 dB Below Carrier
Life Requirements (-1.0 dB)	12 Years (105,000 Hrs.)
Weight	2.5 Pounds, maximum
Length	12 Inches, maximum
Cooling	Conduction
Environmental	TS504550A (Mariner Mars '71)

The large overvoltage design technique requires construction of a multiple pitch helix of high accuracy. Precise turn per inch and helix length control is required. The helix is made in such a way that it is locked into the helix barrel and rod support system precisely as it was wound on its mandrel. This is accomplished with a construction method known as the etched mandrel technique. Because of this precision construction it is possible to duplicate closely the operating voltage requirements from tube to tube, as well as to duplicate efficiency performance.

PPM Focusing

From the standpoint of both thermal heating of the helix and beam efficiency, it is necessary to obtain high performance electron beam focusing. This can be accomplished with the well known PPM-focusing technique. High performance focusing requires a PPM design using large values of plasma wavelength to magnet period ratio ($\lambda_p/L \cong 3.0$). This is necessary to maintain acceptable helix current interception under the large electron velocity spread which occurs under high efficiency conditions. A direct consequence of these criteria at X-band is that high-coercive-force magnet materials must be used to obtain the large values of peak magnetic field strength required. Thus, the design uses hybrid magnet stacks composed of samarium-cobalt and platinum-cobalt materials.

Convergent Flow Gun

The convergent flow gun design is determined by three criteria. The first is the value of operating current density to be drawn from the cathode. This is set primarily by cathode operating temperature which in turn is determined by life considerations. The second is the beam current density in the helix region which is set by the combination of design beam efficiency, frequency and power output. The ratio of the beam to the cathode current density determines the required area convergence ratio of the gun design. The third criterion is set by the required gun perveance ($I/V^{3/2}$), where I is cathode current and V is the anode voltage. To prevent ion drainage into the cathode, the gun perveance should be less than the beam perveance of the tube so that the anode voltage is higher than the helix voltage.

In view of the very long life goals of this tube, a relatively new cathode material which has high current density capabilities as well as excellent promise of the required long life capability will be used. This is the Coated Powder Cathode.[3] This material is capable of delivering up to 2.5 to 3 times the current density at the same operating temperature as the normal oxide cathode. This allows a smaller area convergence ratio of the electron gun which implies, in general, better beam laminarity at the beam minimum diameter and allows the minimum to occur at a greater distance from the anode of the gun. This latter property greatly facilitates achieving proper entrance conditions into the magnetic focusing structure.

Two-Stage Collector

A two-stage collector, with its attendant greater complexity, must be used to achieve the required high overall efficiency. The greater efficiency improvement ratio of the two-stage collector over the single-stage collector is necessary to compensate for the lower beam efficiency achievable at X-band. To achieve the improved efficiency performance, the collector must internally sort the electrons so that they can be collected at lower potentials. It must also maintain control over secondary electrons and reflected primary electrons to prevent them from reaching the helix and dissipating their energy at its higher potential. The internal design of the collector determines whether it performs these functions or not. This is a crucial part of the design and is necessary to meet the efficiency goals. Past history of two-stage collector performance has not been good despite much theoretical analysis showing that it is possible. Currently, some new ideas for the design coupled with computer analysis techniques for solving electron trajectories is making it possible to achieve previous expectations.

Major Development Problems and Status

Most of the development problems arose from the dimensional and electrical scaling from S-band to X-band. The ratio of the S- to X-band frequencies is 3.7:1. If the scaling were carried out holding helix γa and beam perveance constant at the same power level, this would also be the ratio of the helix diameters. However, because of focusing and certain mechanical limitations, the perveance was decreased.

Construction

Problems of construction and assembly of the helix and placing it accurately into the surrounding barrel proved to be very difficult. This was solved satisfactorily after considerable effort and allows repeated and accurate fabrication of the precision multiple pitch helix and barrel assemblies.

Special problems were encountered in brazing the completed barrel-helix assembly to the large polepiece assemblies at the gun and collector end of the tube. The barrel with the assembled helix inside must be brazed to the polepiece assembly without damage to the helix and rod structure which passes inside the barrel beneath the point at which the braze is made. This braze is a vacuum seal and thus is critical to achieving a working tube.

Joining the input and output coaxial lines to the helix proved to be a very difficult operation. The point where the helix and the coax join are almost inaccessible. In addition, the joining operation must be performed so that the helix is not distorted in any way which would make it move into the region of the electron beam and cause helix interception.

These assembly problems were solved by using the procedures described later.

Electron Beam Focusing

The major beam focusing problem which was encountered involved the proper entrance of the electron beam into the helix. This was only partially solved during the course of the program and prevented operation under CW conditions at full beam current. This resulted from the use of an existing electron gun design in an attempt to conserve project funds. In the long run this turned out to be a poor choice. The solution to the problem is to redesign the electron gun for higher perveance to realize optimum electron beam entrance into the helix and magnetic field region. In addition, it might be necessary to decrease the beam perveance, or conversely, to increase the peak magnetic field.

Achievements

Construction

Four (4) PPM-focused RF tubes and one (1) PPM-focused beam tester were built during the course of the program after the early construction problems were solved.

Tube

S/N 1	4 rod helix, single-stage collector
S/N 2	3 rod helix, two-stage collector
S/N 3	3 rod helix, two-stage collector
S/N 4	Beam Tester: 3 rod helix attenuated over entire length, no RF connections, single-stage collector
S/N 5	3 rod helix, two-stage collector

RF and Focusing Performance

Power output of 25 watts was achieved. This was measured only under pulsed conditions because of the limitations on the dc focusing into the helix at the operating helix voltage and current necessary for this power level.

A best value of beam transmission of 96 percent was achieved on S/N 5 under dc conditions at 50 mA of cathode current. This was accomplished at the design helix voltage of 2250 V. The actual operating conditions for the 25 watt power level were 2100 V at 50 mA. Unfortunately, the focusing performance had deteriorated sufficiently at this lower voltage so that the tube could not be run under dc or CW conditions.

Several tubes exhibited saturated gain greater than 30 dB. Gain is not considered a problem since it can be adjusted to any desired value by changing the length of the input helix once the output helix design and performance have been established. Adjustments in gain can be made independent of power output and efficiency.

Beam efficiency of 21.5 percent was achieved. This was based upon measured power output and calculated using the dc beam current transmitted through the helix and ignoring the current intercepted by the helix. Most of the helix current interception occurred at the entrance to the helix and was the result of improper beam entrance conditions; RF defocusing caused some of the interception, but this was of less significance. This efficiency value has not been optimized at this point by adjustment of helix parameters. Large signal calculations, as well as S-band data on other tubes under similar operating conditions, indicate that 28 percent beam efficiency is achievable. This can be achieved by optimizing helix length and phase velocity and probably will be realized during the construction of a few more experimental tubes.

Present Status of Design

The first five tubes served as vehicles to work out mechanical and electrical construction problems. This phase has been essentially completed. These tubes also served to test the focusing system and allowed the identification of the focusing problem and have pointed the way to the solution of the problem.

Recommendations

The next step is to redesign the electron gun for a gun perveance of about 0.4 micropervs. This will lower the anode voltage and thus tend to eliminate the strong electric lens which now exists in the gap between the anode and helix. This lens has caused excessive beam scalloping at the helix entrance. The scalloping has been only partially compensated by the magnetic lenses at the beginning of PPM focusing structure. It is estimated that the redesign of the gun would allow dc transmission of 98 to 99 percent to be achieved under full dc operating conditions. Under CW RF conditions, a transmission of at least 93% should be achieved.

Following the gun redesign, a series of tubes should be built with engineering design changes to determine the correct helix length, helix pitch and pitch changes along the helix. These tubes could also incorporate any design changes necessary to the two-stage collector to optimize its performance.

III. DETAILED DESCRIPTION OF DEVELOPMENT PROGRAM

Basic High Efficiency Approach

At S-band (2.3 GHz), two basic tube types have been developed using large overvoltage design techniques. The lower power type, the WJ-274 family, delivers greater than 40 percent overall efficiency at 9.0 watts output and 45 percent efficiency at 28 watts. The higher power type, the WJ-395 family, delivers 45 percent efficiency at 50 watts output and 47 percent efficiency at 100 watts output. This is performance which is typically achieved with encapsulated, deliverable tubes. Individual tubes operating under optimized test bench conditions have given as high as 51 percent overall efficiency (a WJ-395 at 100 watts output).

These designs could be scaled directly to X-band by maintaining the helix parameter γa and the beam perveance at the same values as the S-band tubes. This would lead to impractical designs however. By allowing the beam perveance to drop from the value of 0.8×10^{-6} of the S-band tubes to 0.65×10^{-6} for the X-band design, the electron beam can be focused using the new high coercive force permanent magnet material, samarium-cobalt. The mechanical design of the helix at this perveance value is impractical, however, because the required diameter of the beryllium oxide ceramic support rods for the helix is too small. Centerless ground BeO rods of 0.010 inch diameter would be required and these would be too fragile to manufacture in the required lengths and too fragile to handle in the subsequent tube construction.

Allowing the beam perveance to drop to the value of 0.45×10^{-6} permits the use of BeO ceramic rods which are 0.024 inch in diameter. This is a practical size to manufacture and handle. The magnet material can now be either platinum-cobalt or samarium-cobalt material. The consequence of the beam perveance value of 0.45×10^{-6} is that the maximum beam efficiency which can be reached is reduced to 28 percent from a value of 36 percent. The need for the two-stage collector with a larger efficiency improvement ratio than the single-stage collector is apparent.

The large overvoltage design requires the correct combination of certain basic TWT parameters such as γa, QC, b, d, CN and b/a. These design parameters are listed in Table II. Electron beam interception on the helix under large signal conditions is a function of the beam perveance. Large signal interception decreases as perveance is reduced. The percent beam transmission for the 0.45×10^{-6} perveance design under large signal conditions should be better than that of the S-band tubes.

TABLE II

DESIGN PARAMETERS

Output Circuit Parameters*	
γa	1.13
QC (Space Charge Parameter)	0.159
b (Velocity Parameter)	2.83
d (Loss Parameter)	0.05
CN	1.33
Beam Parameters	
Perveance, P_{Beam}	0.4×10^{-6} $A/V^{3/2}$
$b/a \left(\frac{\text{Beam Radius}}{\text{Helix Radius}} \right)$	0.4
Predicted Performance (Based on large signal computer calculations)	
Power Output	31.7 watts
Beam Efficiency	28 Percent
Overall Efficiency (including heater power and two-stage collector)	49.3 Percent

* See Reference 4.

Magnetic Design

In the previous section, it was indicated that the choice of larger diameter helix support rods had an impact upon the perveance of the electron beam which could be focused. This results from the fact that the diameter of the helix barrel is determined by the diameter of the helix plus the diameter of the rods. The inside diameter of the magnet polepieces is set by the outside diameter of the barrel. Thus, larger diameter rods means the polepiece inside diameter is farther from the axis and the peak magnetic field on the axis is lower for a given magnet period. The beam perveance which can be focused is a function of the peak magnetic field which is obtained.

In the small signal region of the helix, i.e., all of the helix except approximately the last 0.7 inch of the output helix section, the electron velocity spread is small and good focusing can be obtained with a magnet period of 0.150 inch. This corresponds to $\lambda_p/L = 2.6$. Under these conditions, a peak magnetic flux density as high as 2250 gauss can be obtained with platinum-cobalt material.

In the large signal region of the output helix, the electron velocity spread increases greatly and the magnet period must be shortened to 0.134 inch to maintain good focusing under these conditions. This corresponds to $\lambda_p/L = 3.0$ and Samarium-cobalt is required to reach 2250 gauss.

At the time that this program was begun, Sm-Co was a new and little tried material. It presented difficulties in magnetization and demagnetization because of its high coercive force and straight line demagnetization curve. Standard magnet treating equipment was inadequate and special equipment had to be obtained. The material was far too strong for the longer magnet period in the small signal section of the tube. To use it required too great a demagnetization from its saturated value. It became clear that what is really needed in this section of the tube is a version of rare-earth magnet material with the characteristics of platinum-cobalt. This would satisfy the majority of the magnet requirements and not be so difficult to handle.

During the course of this program, the cost of samarium-cobalt magnets decreased from a value equal to that of platinum-cobalt to one-half of that cost or less depending on quantity. Further price reductions appear probable in the future and the magnet manufacturers have been alerted to the requirement for a version with a lower coercive force.

Helix Design

To give the helix the best heat dissipation capability for the 50 watt mode requirements which existed at the beginning of the program, it was decided to use a four rod helix support. This increases the number of heat paths from the helix to the barrel from three to four. It also cuts down the maximum heat path length along the helix tape from 1/6 of a turn to 1/8 of a turn. Both of these factors help to reduce the maximum temperature of the helix under a given power dissipation situation.

The dielectric loading of four rods is greater than a conventional three-rod structure, so the initial design was based upon a best estimate of this factor. A helix was built according to this design and it was found that the dielectric loading factor was greater than anticipated. The helix was then redesigned to take this into account.

Construction difficulties were encountered for a helix-rod-barrel structure suitable for use on an actual tube. These problems had mainly to do with size but were also complicated by the requirement for four rods. The deformation of the barrel to allow helix insertion becomes much more critical with the four-rod structure and can more easily pass the elastic limit of the barrel material.

In the meantime, because of the funding limitations imposed on the program, the maximum power output requirements were reduced from 50 to 25 watts. This decreased the thermal loading on the helix by a factor of 2 and it was decided to return to the three-rod structure with its less critical assembly procedure for all tubes subsequent to S/N 1, which was built with a four-rod helix.

At this point in the tube construction, a change in the dielectric loading to that of the three-rod structure could have had a major impact on the helix and body design. Materials and parts were on hand and designs were complete. It was also desirable to keep the barrel and magnet design of the four-rod structure if possible. This would allow a return to 50 watt operation at some future time if the system requirements so warranted. This could be done at a minimum cost if the body and magnet diameter did not have to be changed. For these reasons, it was decided to construct a three-rod helix with the same dielectric loading as that of the four-rod helix which would fit into the same barrel diameter. This was accomplished by using rods of a larger diameter which had flats ground longitudinally along one side so that the distance through the rod from the flat to the opposite side was the same as the original round rods.

The flat side was placed against the helix. This effectively increases the amount of dielectric in the proximity of the helix and increases the dielectric loading. Curves showing normalized phase velocity vs. normalized frequency for the three- and four-rod structures are shown in Fig. 1.

The design dimensions and the electrical parameters are given in Table III.

Assembly Procedures

Helix Assembly

A typical helix for a large overvoltage design TWT will consist of three distinct sections. This helix will be wound continuously on one mandrel with pitch changes in the helix at the appropriate positions. The input helix section will consist of a uniform TPI from the beginning to the center of the helix attenuator. The main output section begins at the center of the attenuator and extends at a constant TPI to the beginning of the output taper section. Depending on the design, the output taper may consist of a gradual change in TPI to the end of the helix or may consist of an abrupt change in TPI which is then held constant to the end. The length of each individual section of the helix is critical to the overall efficiency, power and gain performance and accurate helix winding techniques must be employed.

To guarantee that the helix remains on the mandrel through the subsequent operations precisely as wound, the mandrel is plated with a brazing alloy before winding. After winding, the helix is fired in hydrogen so that the alloy flows and the helix is brazed to the mandrel. This then gives a rigid structure that can be centerless ground on its outside diameter. This removes the imperfections of the helix tape and the outside surface of the helix lies on a true cylindrical surface. This will provide an optimum thermal contact to the ceramic rods which will later press against this outside surface. At this point, the helix can be precisely trimmed to length on the mandrel and the end helix turn can be precisely cut with respect to the winding transition points on the helix.

At this point the helix must be inserted into the metal barrel with the ceramic rods and locked into a precise longitudinal and rotational position. Achieving this step required a major effort during the helix development phase. It was found, for instance, that the ceramic rods could not be held accurately in place during insertion by the same jigging arrangement as at S-band. The dimensions of the parts were simply too small.

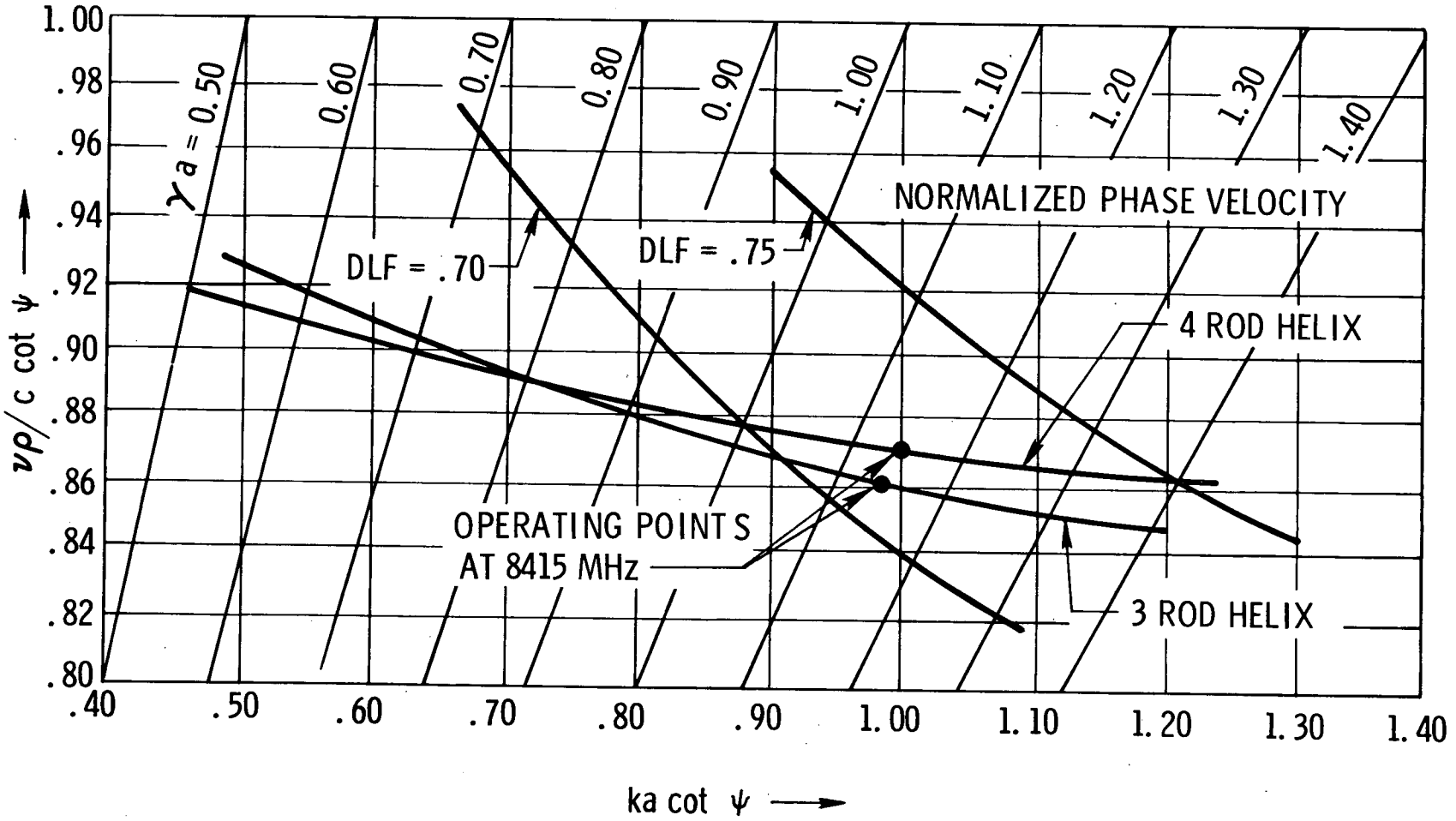

Fig. 1 - Normalized phase velocity vs. normalized frequency for helix designs with 3 and 4 rod dielectric supports. The 3 rod structures use flats on the rods to match the dielectric loading of the 4 rod structure.

TABLE III

WJ-3703 CHARACTERISTICS

MECHANICAL

Helix Diameter (I. D.)	0.0334 inch (.0848 cm)
(O. D.)	0.0414 inch (.105 cm)
Output Helix TPI	100 turns per inch (39.4 TPC)
Tape Width	0.006 inch (.0152 cm)
Barrel Diameter (I. D.)	0.0889 inch (.226 cm)
(O. D.)	0.0995 inch (.253 cm)
BeO Rod Diameter	0.0271 inch (.0688 cm) with a flat on one side which gives a reduction in diameter of 0.003 inch (.00762 cm) (See Fig. 3)
Polepiece (O. D.)	0.520 inch (1.32 cm)
Thickness	0.020 inch (.0508 cm)
Magnet Thickness (Platinum Cobalt)	0.060 inch (.152 cm)
(Samarium Cobalt)	0.047 inch (.119 cm)
Magnet I. D.	0.140 inch (.356 cm)
Spacer Magnet Thickness	0.080 inch (.203 cm)
Coupler Magnet Thickness	0.132 inch (.335 cm)
Cathode Diameter	0.172 inch (.437 cm)

Design Values

Beam Diameter	0.0155 inch (.0394 cm)
Cathode Beam Area Convergence	123:1

ELECTRICAL

Helix Voltage	2250 V
Body Current	3.5 mA
First Stage Collector Voltage	1460 V
First Stage Collector Current	15.5 mA
Second Stage Collector Voltage	1125 V
Second Stage Collector Current	30.0 mA
Anode Voltage	4000 V
Anode Current	10 μA
Gun Perveance	0.194×10^{-6} A/V$^{3/2}$
Beam Perveance	0.46×10^{-6} A/V$^{3/2}$

A technique to hold the rods in place on the helix called the glued rod technique was finally worked out. This consisted of holding the helix and the rods in the precisely correct relationship in a special jig and gluing the rods to the helix and mandrel with a soluble cement. When this is accomplished, the barrel is deformed with a deforming jig, the helix and rod combination are inserted and placed in the correct location and the barrel is released. The cement can then be dissolved out of the structure and the mandrel and brazing alloy are removed by differential etching. This then leaves the helix clamped tightly by the rods and barrel in precisely the desired location and exactly as originally wound on the mandrel. The inward force of the released barrel actually deforms the helix slightly out of round and provides the required pressure necessary for good heat transfer from the helix to the rods and the rods to the barrel.

A photograph of the end view of a four-rod helix is shown in Fig. 2. A similar photograph of a three-rod helix is shown in Fig. 3. Here the flats on the side of the rods in contact with the helix can be seen. A side view of a three-rod helix structure is shown in Fig. 4. The coaxial line connects to the helix through the circular opening in the side of the barrel. The outer conductor of the coaxial line is just the size of the opening. The center conductor extends through the opening and is connected to the end of the last helix turn which is directly below the center of the opening.

Body Braze to End Polepieces

The end polepiece assemblies of the tube are fairly complex assemblies which contain a large polepiece cup which accepts either the gun or the collector, two magnet cells with polepieces, the coaxial line with vacuum window and a central body tubing which telescopes over the helix barrel. These assemblies are furnace brazed together prior to mounting to the helix barrel. The assemblies are then joined to the helix barrel by an RF induction heating braze.

This is a very difficult braze to control because it is in such intimate association with the helix and its support rods. It is very easy to crack the helix support rods during this operation. A break in the rods usually introduces an RF discontinuity on the helix and often ruins its mechanical support. At S-band frequencies where the helix structure is larger, it is possible to place mechanical restraints between the rods and around the helix which will hold them in such a way that the rods are not broken by the forces which occur during the RF brazing cycle. Because of the small dimensions involved, this approach is not possible in the X-band tube. This braze joint must also have reliable vacuum integrity because it is a seal in the vacuum wall.

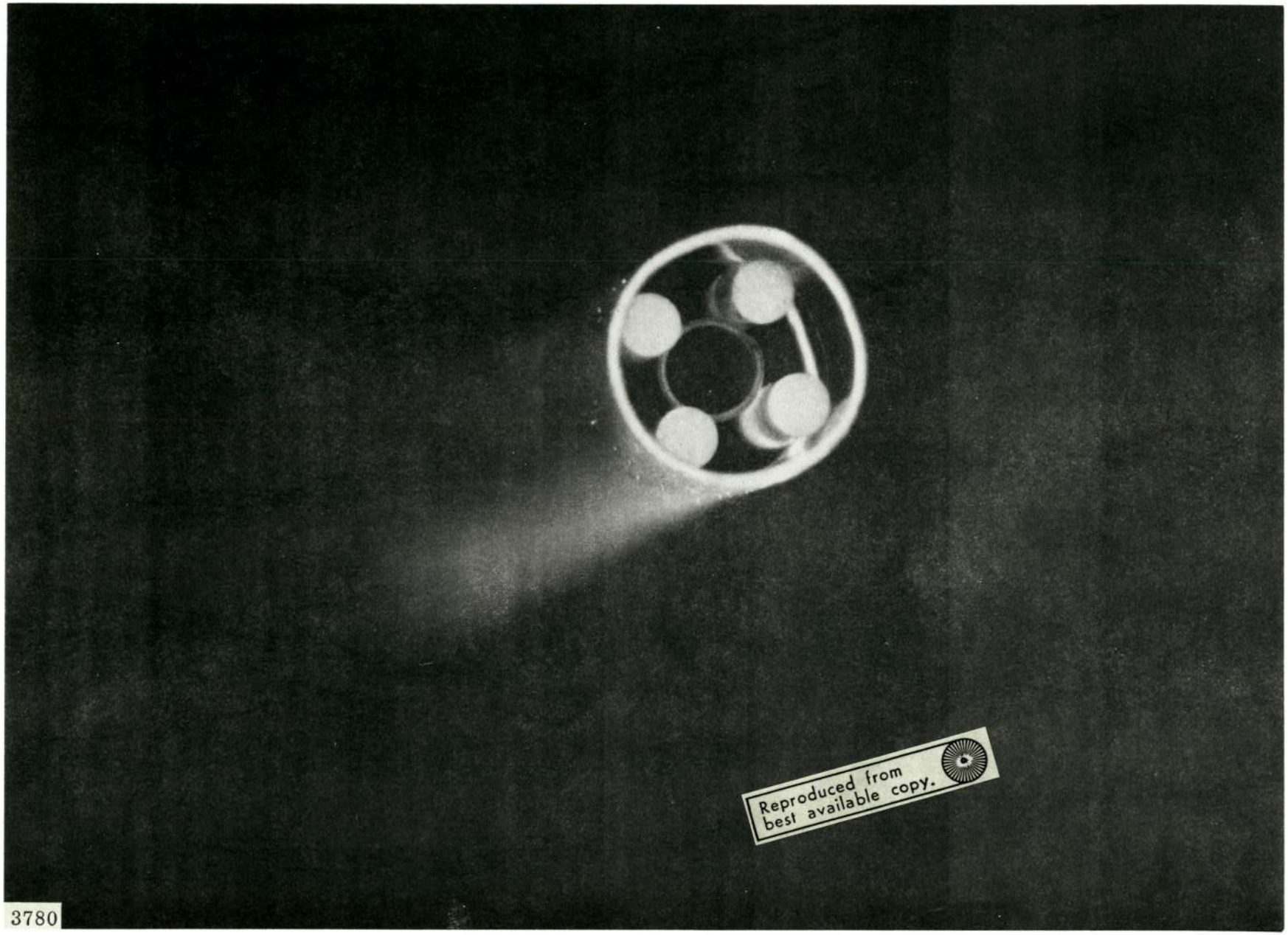

Fig. 2 - End view of a 4 rod helix assembly.

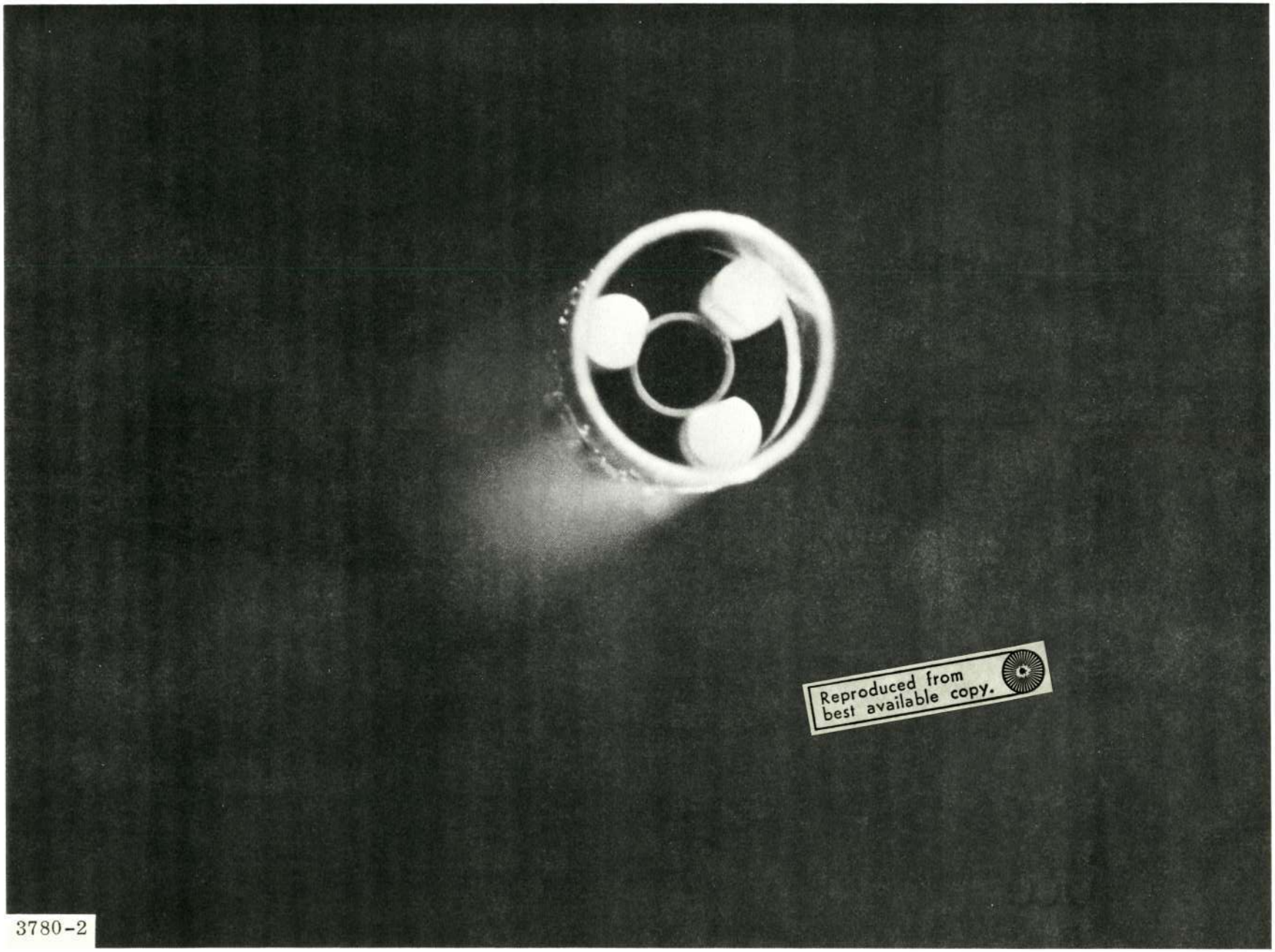

Fig. 3 - End view of a 3 rod helix assembly.

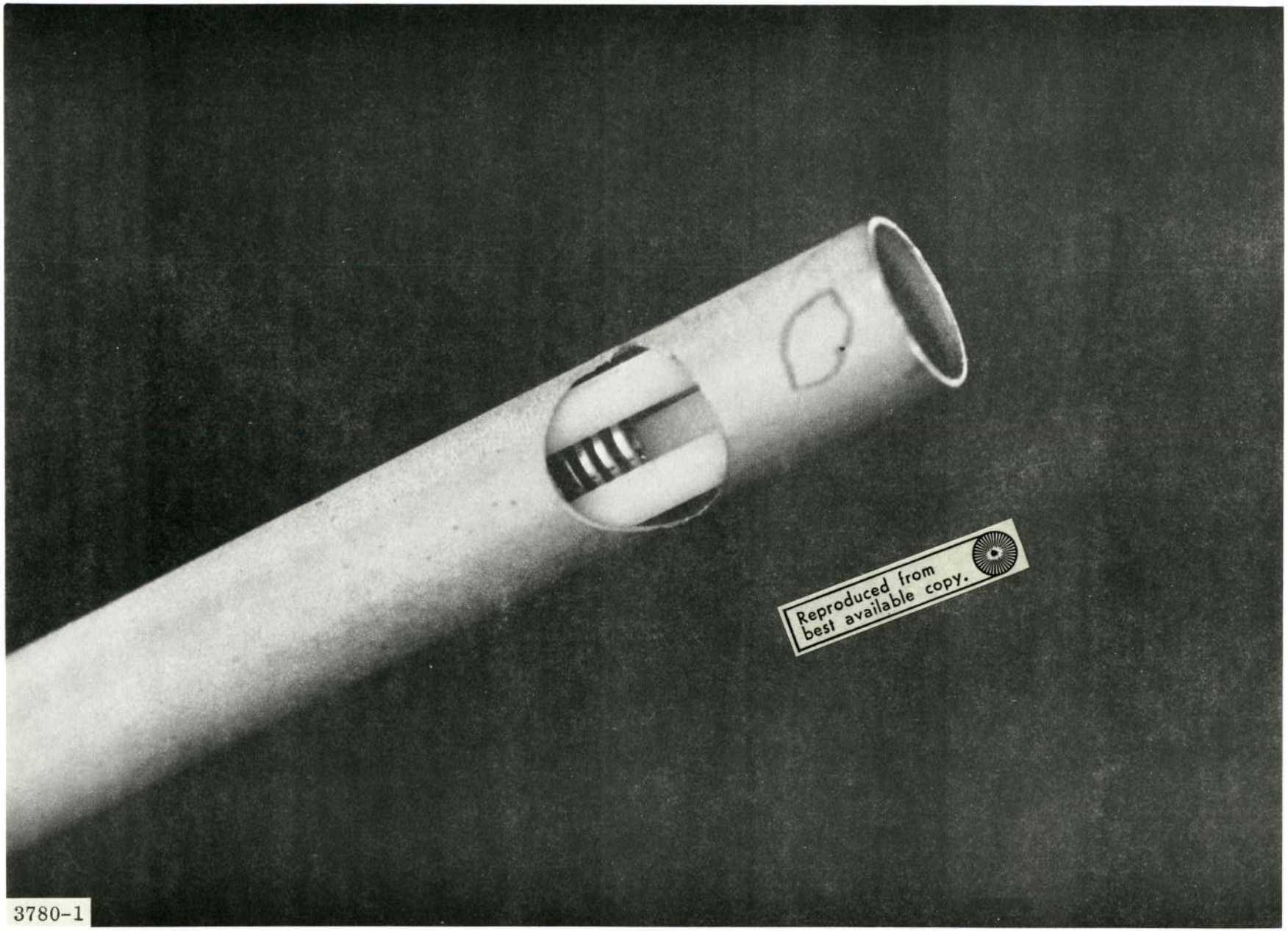

Fig. 4 - Side view of a 3 rod helix assembly showing the circular opening for the coaxial line.

The approach used to achieve a reliable braze still uses RF induction heating. The parts to be joined are carefully designed to allow very rapid heating with a minimum total heat required so that adjacent parts have only a minimal increase in temperature. The braze joint gap is designed to optimize the capillary flow of the molten braze into the heated areas and the surfaces are plated so that good wetting action of the surfaces occurs. The braze is accomplished in a hydrogen bell jar using a special RF concentrator so that the RF fields have tight coupling to the elements to be brazed only in the joint region.

The design of the joint is shown in Fig. 5. It is seen that the body assembly containing the helix is inserted into the polepiece assembly. The completed braze has flowed into the capillary gap and has formed an external fillet. This joint does not have to provide much in the way of mechanical support. This is supplied by the accurate telescoping fit between the helix barrel tubing and the tubing on the I. D. of the polepiece assembly. The braze is accomplished in about three seconds with only the undercut end of the projecting sleeve and the thin-walled body tubing reaching the alloy melting temperature. The helix rods are supported by the cold body sections on either side of the braze location and thus form a bridging support for the helix when the body section expands away during the braze. The high thermal conductivity BeO rods are able to conduct enough heat away to prevent heat shock.

Coaxial Line to Helix Transition

The coaxial line to helix matching system is based upon a quarter-wavelength matching transformer. This is accomplished by bringing a 50 ohm line into the tube through the 50 ohm vacuum window. At a distance of one quarter-wavelength from the beginning of the helix, the characteristic impedance of the line is increased to 134 ohms, which is the geometric mean impedance of the line and helix. The matching region is shown in Fig. 6. The 50 ohm section of line uses a molybdenum center conductor. The 134 ohm section of line uses a tungsten center conductor to provide maximum stiffness for the subsequent welding operation to the helix. A supporting bead provides centering at the point where the center conductor steps in diameter.

The process of accurately welding the center conductor to the helix proved to be the most difficult procedure to be worked out on the tube. The primary reason is the inaccessibility of the welding point from outside of the tube. If welding tips are inserted into the body to reach this point, they completely block the visual access. This critical and delicate weld cannot be done blind. The weld

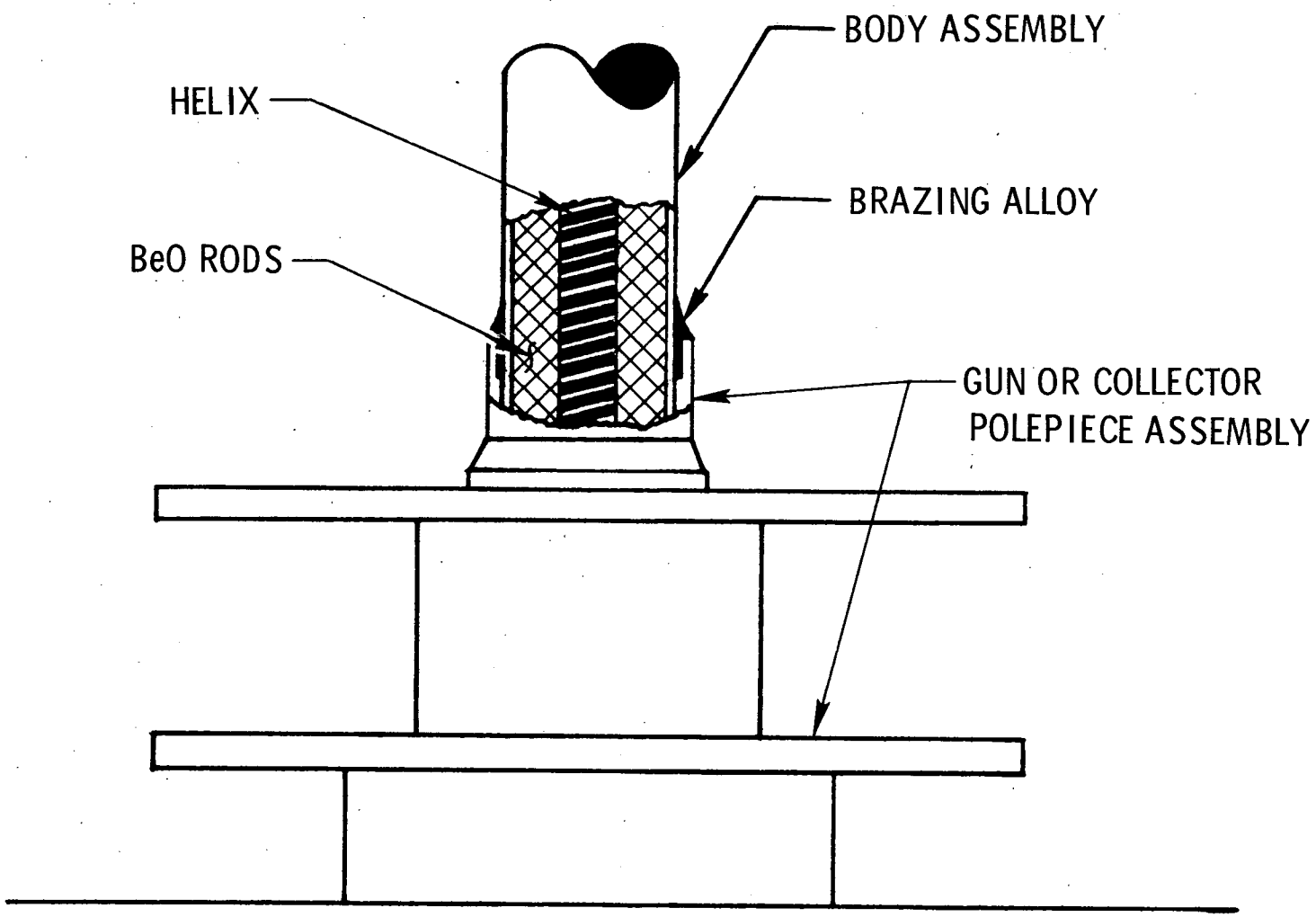

Fig. 5 - Cross-section of the braze joint between helix barrel and polepiece assembly.

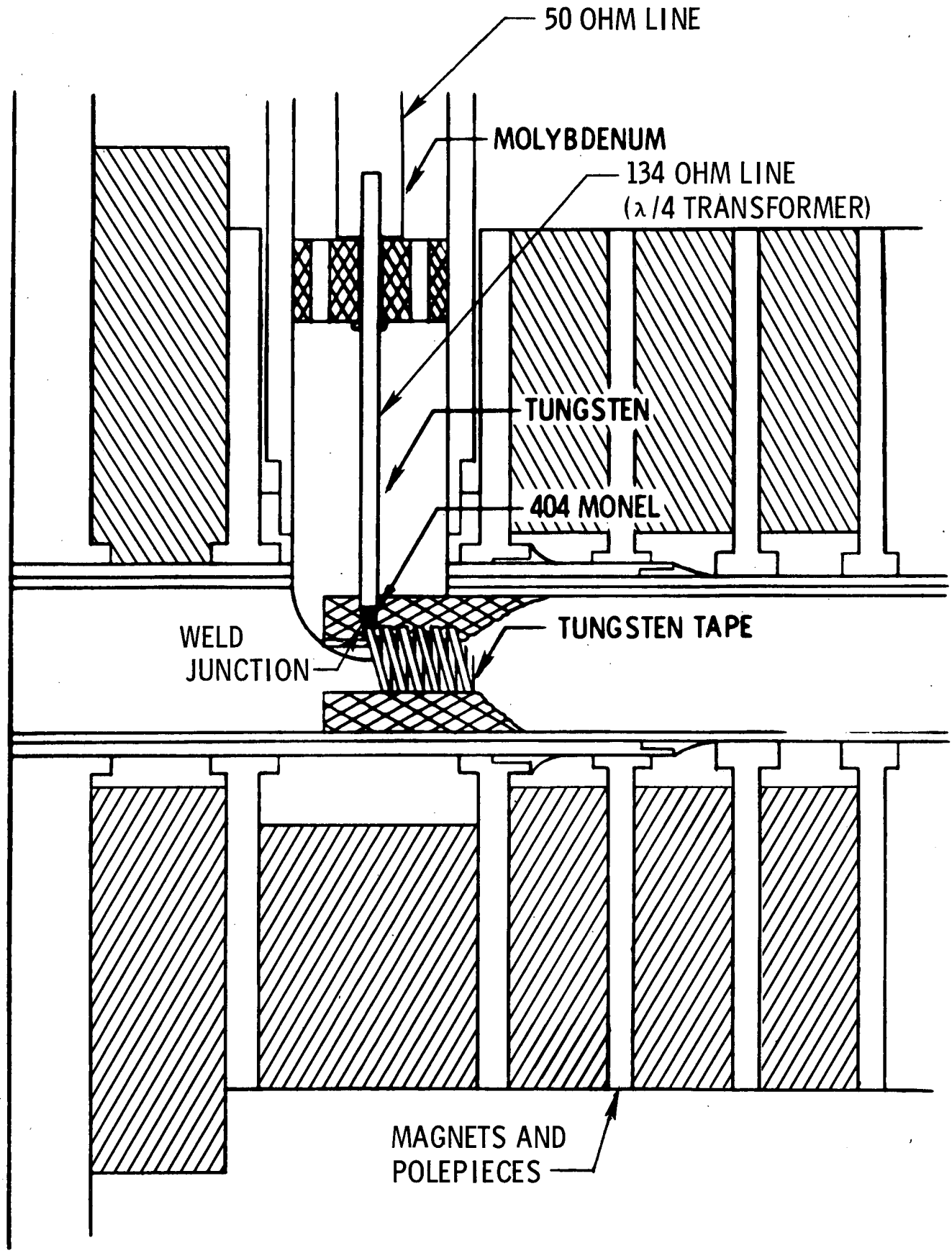

Fig. 6 - Cross-section of the coax to helix transition showing the λ/4 matching transformer and the weld junction.

must also be done so that the helix is not distorted and is not bent into the region of the electron beam. A tight fit of the helix to the rods must be maintained so that heat can be drained out of the helix from the end turns. This is particularly important at the output end.

The weld procedure as finally worked out is begun by preparing the end of the tungsten center conductor with a 404 monel tip. This is melted onto the tungsten and then shaped to provide the correct amount of alloy. The coax center conductor assembly is then lowered into place and the window RF brazed into the window mount. An accurately drawn copper rod which just fits the helix I. D. is inserted from the opposite end of the helix. The current path for the spotweld is through the center conductor to the helix junction and out through the copper rod and back to the welder to complete the circuit. The entire operation is easily visible with a microscope through the open end of the body. Accurate location of the end of the helix and correct length of the center conductor are necessary prerequisites for a good weld. This can be accurately done with this type of assembly procedure.

One problem with the tungsten tape used for the helix is that it will easily delaminate. If the spotweld is made to only the upper surface, a thin section of this surface can later separate from the tape and give an open circuit. This happened to one of the early experimental tubes during bakeout. The monel alloy now used as the spotwelding solder prevents this problem. This results from the very high wetting ability of the tungsten by the monel and the ability of the monel to flow around the tape and mechanically capture it. The resulting spotweld looks more like a braze than a spotweld.

Electron Gun

The electron gun is an electrostatically focused convergent flow design with the magnetic field shielded from the gun region. The design was based upon an already existing design. The perveance of this design was 0.194 micropervs vs. an optimum 0.244 micropervs for a gun suitable for the original dual mode 50/25 watt requirement. It was decided to use this design rather than expend effort on redesign for this small change in perveance. The only change necessary was a dimensional scaling at constant perveance to obtain the desired beam diameter.

When the dual mode requirement was eliminated and the design was optimized for single mode, the beam perveance for the 25 watt mode was shifted from 0.26 to 0.45 micropervs. Since the assumed beam size and minimum position were near the correct values for the 25 watt mode, it was decided to use the same gun design and modify it only slightly. This eliminated a major gun redesign to a gun perveance of approximately 0.39 micropervs. This was not a good decision as it eventually led to focusing difficulties.

This existing design was scaled in dimensions to meet the exact beam diameter at the beam minimum, the parts were built and the design was tested in a gun test bell jar. In this system, a pinhole aperature is scanned across the beam to measure current density. The cross-sectional current density is measured at a number of different planes along the beam beyond the gun anode to determine the beam minimum location and beam spread characteristics.

The effects of minor changes in the electrode dimensions such as variations of the cathode position with respect to the focus electrode and variations of the tip of the reentrant anode sleeve with respect to the cathode were evaluated by making a series of rapid changes in the bell jar. This was done without removing and recoating the cathode by letting it down to atmospheric pressure in a dry nitrogen atmosphere and keeping the cathode warm by leaving 2 volts applied to the heater at all times. This latter procedure prevents moisture pickup by the cathode coating and allows reactivation after the cathode is again in a vacuum. Since these gun tests were made under pulsed conditions, this procedure could be repeated several times before cathode degradation prevented re-use of the cathode. This could always be checked by measuring beam current vs. anode voltage to determine if the cathode was operating space-charge limited.

Fig. 7 shows a computer calculation of the electron beam resulting from the electrode geometry with the design voltages applied. The shortcoming of the computer calculation is that it does not account for the thermal electrons which become very important in large area convergent guns. In the bell jar measurements the beam size was always larger than the computer calculated values. It was found that it was necessary to design for a smaller beam size with the computer so that the measured beam would come out to the desired size. Table IV gives the parameters of the gun finally used.

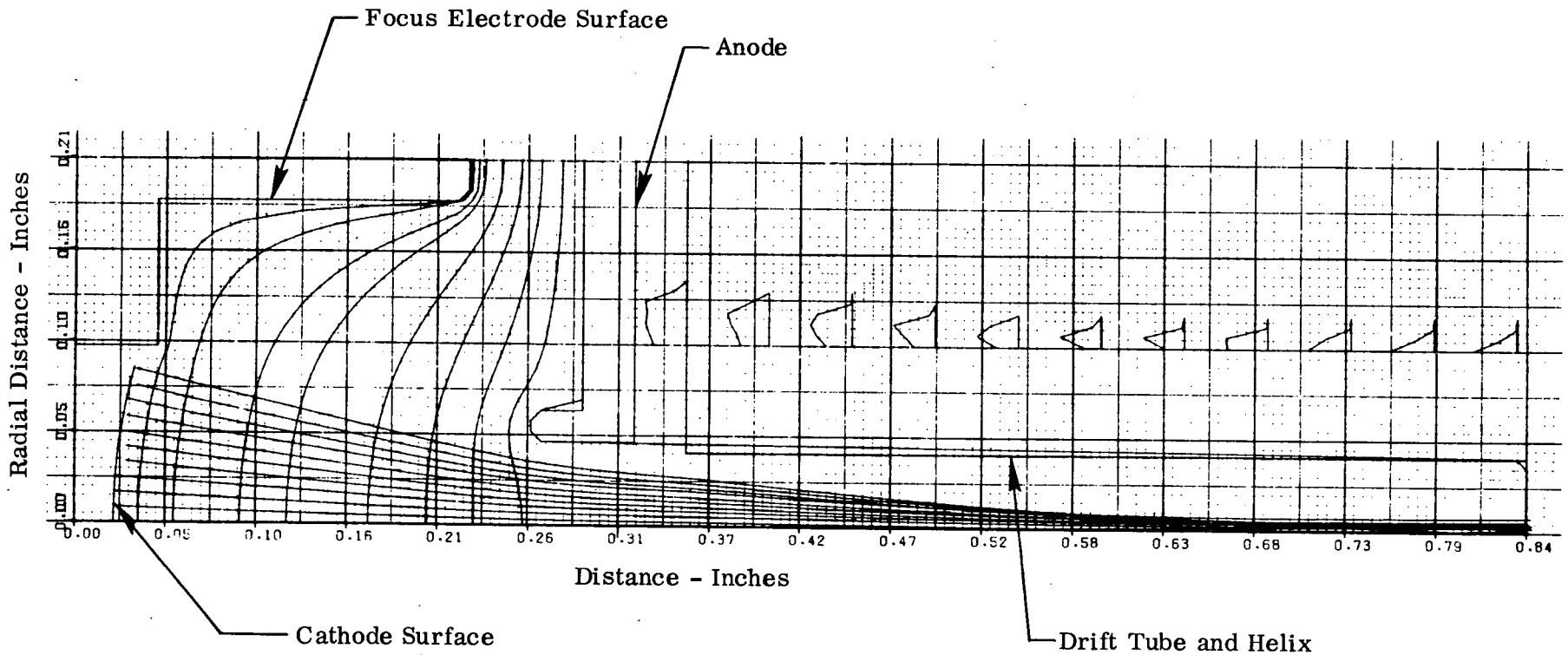

Fig. 7- Computer calculations of electron trajectories in the gun for a 50mA beam.

TABLE IV

GUN PARAMETERS

Gun Perveance	0.194×10^{-6} A/V$^{3/2}$
Cathode Diameter	0.172 inches (.437 cm)
Cathode Current Density	
@ I_o = 50 mA	0.335 A/cm^2
@ I_o = 75 mA	0.54 A/cm^2
Anode Voltage	
@ I_o = 50 mA	4050 V
@ I_o = 75 mA	5300 V
Area Convergence (including thermal electrons)	132
Cathode Type	Coated Powder Cathode (CPC)

For meeting the long life requirements, the Coated Powder Cathode $(CPC)^3$ technology was proposed. This material can give up to 1.0 A/cm^2 continuous current at temperatures below 800°C. A maximum current density of 0.54 A/cm^2 was chosen in the design of the gun to allow operation at a cathode temperature as low as 760°C. At a temperature of 800°C, emission material depletion calculations based upon CPC material on a 0.1% zirconium-nickel base material shows that 90 percent depletion should occur at a time of 100,000 hours of operation. Operating at a temperature between 760°C and 800°C should allow reaching this lifetime on an even more conservative basis. Ion blocking is also employed on these gun designs to prevent ion bombardment of the cathode. This is necessary to prevent destruction of the emission properties of the cathode coating before the potential long life properties of the cathode material can be achieved. This is easily accomplished by designing the anode voltage to be above the helix voltage (gun perveance lower than beam perveance).

Two-Stage Collector

Electrical Design

The depressed collector is used to collect the spent beam electrons at a potential lower than the helix to improve efficiency of the tube. In the case of the single-stage collector, the limitation on the amount of voltage depression that can be applied is the current returned from the collector to the helix and often also to the anode. As the collector voltage is lowered to decrease the dissipation at the collector, there is a point where the increase in dissipation at the helix and anode occurs at a faster rate. This determines the collector voltage at which maximum efficiency occurs.

Two-stage collectors should allow a second electrode to be depressed to an even lower voltage than the first-stage electrode. The lower voltage electrode should then collect the faster electrons in the beam with a resulting lower overall dissipation and higher overall efficiency. In practice, the difficulty which has occurred with two-stage collectors is that the slower electrons do not necessarily end up on the higher voltage electrode. Instead, many electrons (particularly slow secondaries from the lower voltage stage) are focused back out of the entrance tunnel of the collector onto the helix. The result is that efficiency improvement over the single-stage collector has not been significant.

Recently, some new ideas on the internal design of the two-stage collector plus the ability to calculate electron trajectories in the collector with a computer analysis, which takes into account both space charge and electron velocity spread of a spent TWT beam, has allowed the potential efficiency improvement of the two-stage collector to be realized.

Fig. 8 shows a typical wall boundary in the critical entrance region of the collector. This structure has axial symmetry about the lower axis. The electron beam plot shows only 10 electrons to avoid confusion, but the calculation actually was performed with 25 electrons. Their velocity distribution was based upon a 25 electron large signal TWT calculation for the 25 watt case. The internal region of the second-stage electrode has about twice the inside diameter of the first stage and is about four times as long. This is chosen so that the entrance opening into the second stage subtends a small angle from any point on the surface inside the second stage. This opening also has a diameter which is smaller than the inside diameter of the first stage. This tends to shield the interior of the second stage from the potential of the first stage. Thus, the slow secondaries given off of the inside surface of the second stage do not see a large accelerating field toward the entrance. Those returned electrons which do pass through the opening see the relative positive potential of the first stage and are accelerated toward it. Few secondaries and reflected primaries are focused out of the entrance of the first stage and onto the helix.

The resultant performance as the second stage of the collector is depressed below the first stage is a redistribution of current between the two electrodes, with essentially no current emerging from the entrance to be dissipated on the helix. With the first stage operating at a voltage corresponding to the normal optimum point of a single-stage collector, any reduction in the second-stage voltage represents an improvement in overall efficiency. Calculations based upon the velocity and spatial distribution of the electrons in the collector predict that an overall efficiency of 49.5 percent could be achieved with a beam efficiency of 28 percent at the 25 watt level.

Thermal Design

This collector is designed to be conduction cooled to the capsule. The two stages are nested concentrically with the heat from each stage brought down to the capsule base through copper feet. A photograph of the collector is shown in Fig. 9. It is seen that the two stages are insulated from one another by a cylindrical ceramic insulator.

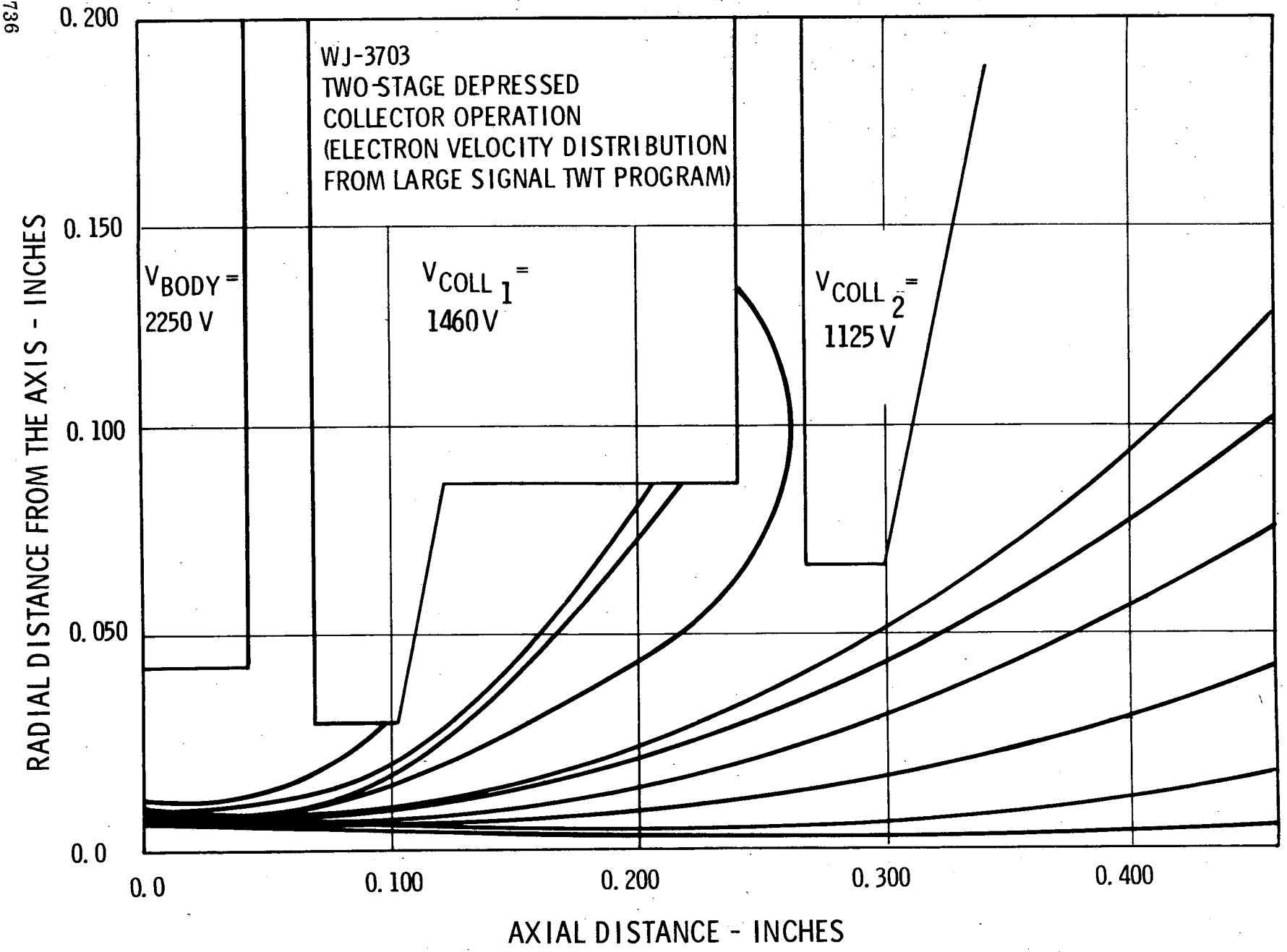

Fig. 8 - Electron trajectory calculation in the two-stage collector showing current distribution of a 50 mA beam.

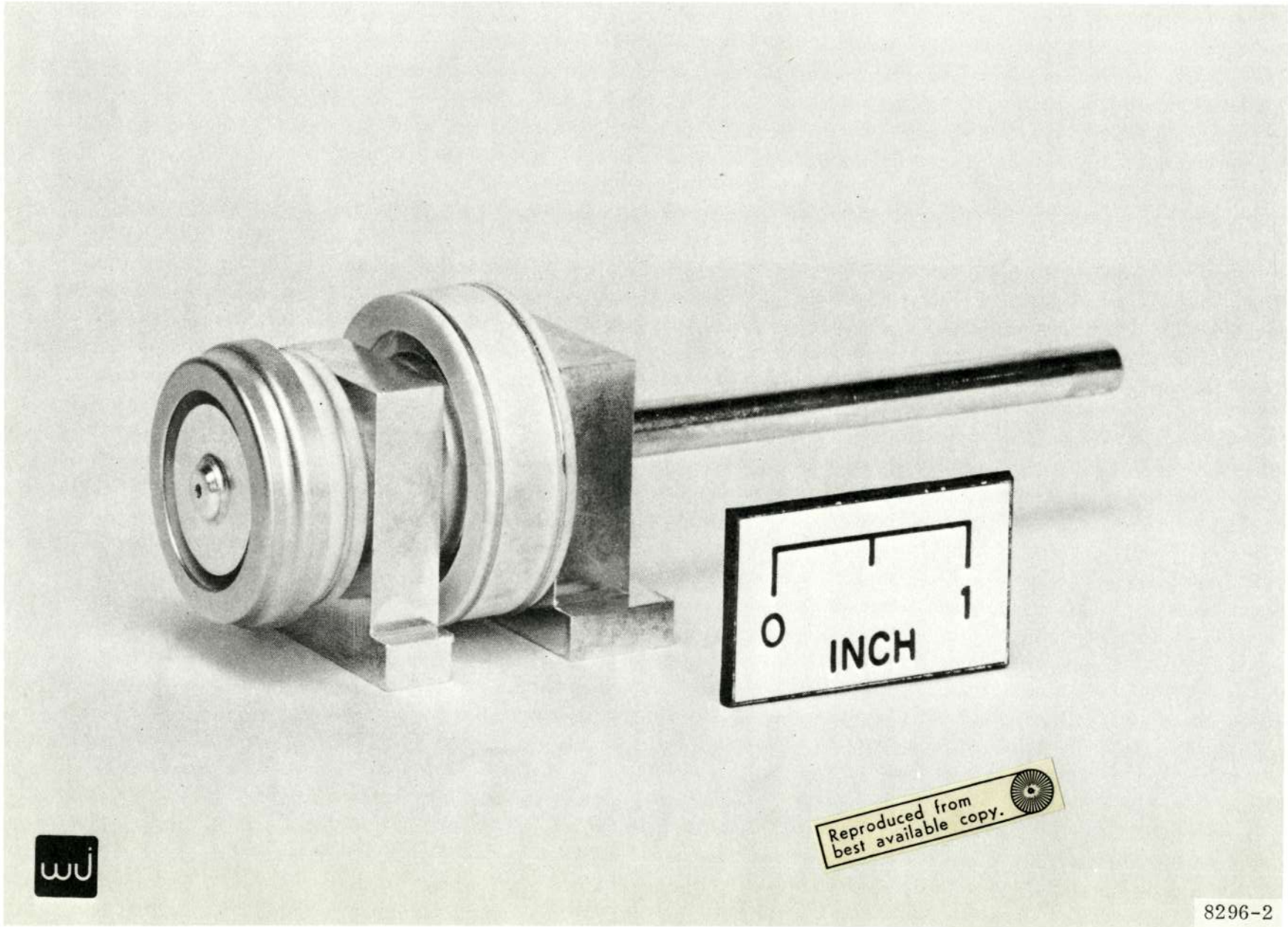

Fig. 9 - Photograph of the 2-stage conduction cooled collector.

The bottom of the two feet lie in the same plane and these will rest on a rectangular beryllium oxide plate the lower surface of which is in contact with the inside bottom surface of the capsule. The microscopic voids between the metal and ceramic will be filled with a silicone elastomer potting material thereby guaranteeing good thermal contact even under high vacuum conditions.

The feet are held by pressure against the ceramic by a force pushing from the top of the capsule. The volume surrounding the collector and ceramic is filled with elastomer which is bonded to all the tube surfaces. This provides the high voltage insulation under vacuum conditions. This general heat transfer design has been proven with S-band tubes to be able to handle several hundred watts of thermal power with low temperature drop from the collector hot spot to the baseplate.

The vacuum pump out is through the end of the collector. Ion blocks are built into the vacuum path to keep the ion beam out of the collector pinchoff.

Overall Tube Design

An overall cross-section of the metal-ceramic tube envelope construction is shown in Fig. 10. Details of the gun, coaxial matching system, magnets and collector are shown. The gun and collector are built as separate assemblies and then are joined to the main body of the tube by RF induction brazing. The cathode is a separate assembly within the gun which is coated and assembled into the tube last. It is also easy to remove the cathode assembly and recoat it for any subsequent reprocessing of the tube.

A photograph of an assembled and processed tube with magnets in place and ready for test is shown in Fig. 11. The connectors are 3 mm OSM type and protect the vacuum window from stress of connection and disconnection.

The tube will be mounted in a capsule whose outline and dimensions are shown in Fig. 12. The weight of the capsule and tube would be 2.6 pounds with an aluminum capsule and 2.0 pounds with a magnesium capsule. The high voltage terminals will be insulated from the capsule by a silicone elastomer which has been vacuum potted into the voids between tube and capsule. All high voltage surfaces will be coated with silicone primer to avoid any lifting of the potting material under vacuum conditions which invariably leads to voltage breakdown. The tube will be supported within the capsule to allow it to meet vibration, shock and

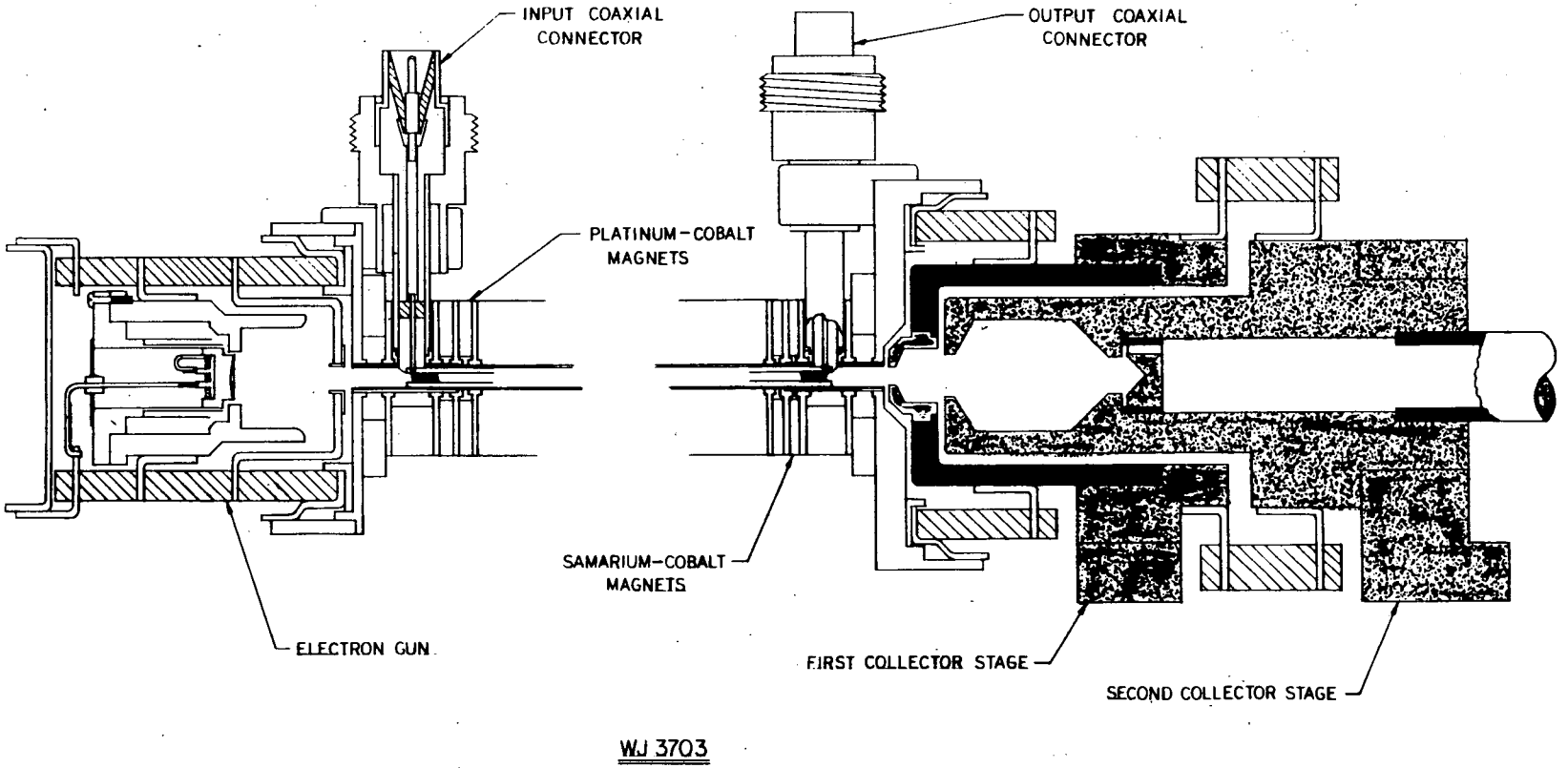

Fig. 10 - Cross-section of the tube showing details of the various tube assemblies.

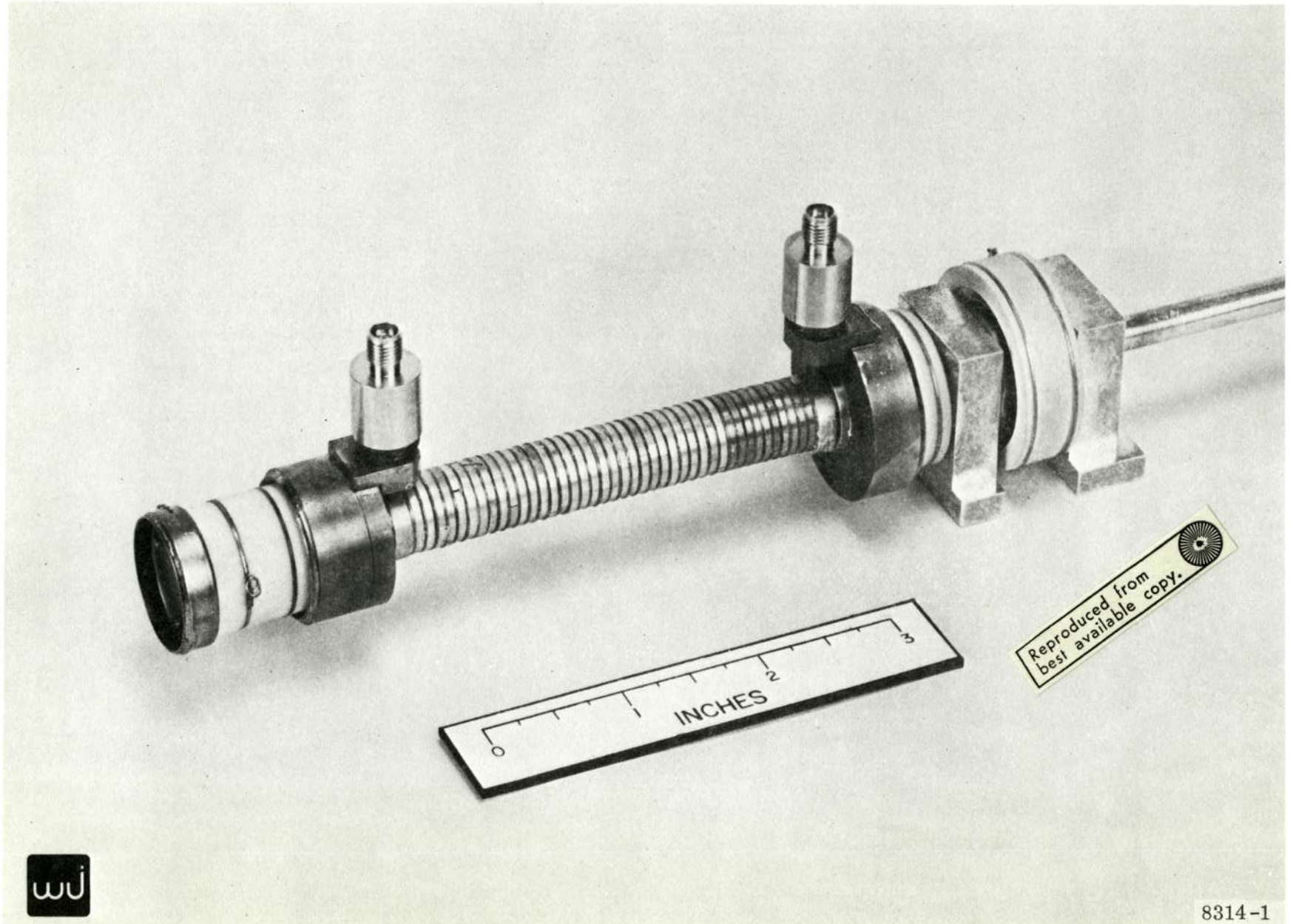

Fig. 11 - Photograph of an assembled tube which is processed and ready for test.

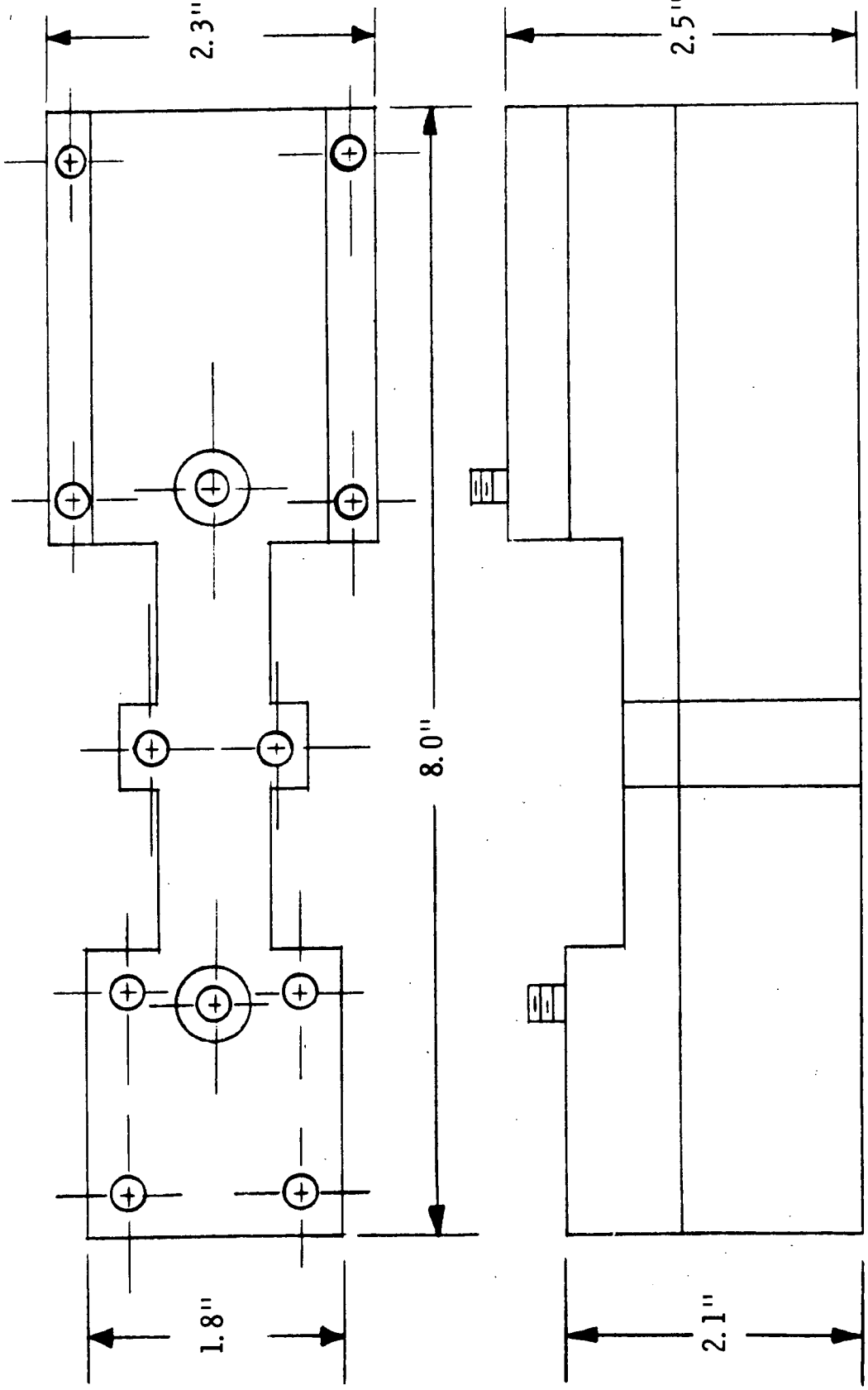

Fig. 12 - Outline dimensions of capsule which would contain the tube of Fig. 11.

temperature conditions. The collector will be the anchor point to the capsule. Any differential expansion vs. temperature between tube and capsule will be taken up by longitudinal motion at the gun. The gun will be supported so that transverse vibrational motion is damped but longitudinal sliding motion is allowed. This encapsulation technique has been thoroughly tested and evaluated on S-band 50 and 100 watt tubes.

SUMMARY OF ACCOMPLISHMENTS IN DESIGN AND CONSTRUCTION

The major portion of the effort was spent in overcoming major assembly problems due to scaling the S-band high efficiency design to X-band. This resulted from a 3.7:1 frequency scaling and an approximate 3:1 diameter scaling. Several difficult constructional problems were solved. The difficulty of some of these problems had not been anticipated. The following list indicates the principal problems solved:

1) Accurate X-band helix assembly technique with variable pitch helices locked into the body as wound.

2) Development of a four-rod helix assembly designed for handling of a 50 watt power level through improved conduction cooling paths. This structure was never tested under this power level of operation, however.

3) Development of the capability of brazing the helix assembly to the end assemblies without damage to the helix during the process.

4) Construction of a rod supported helix structure which could pass through bake-out without damage to the rods or distortion to the helix.

5) Development of a technique for connecting the coaxial line to the helix. This was a very difficult problem because of the small size of the helix and body, the inaccessibility of the junction, and metallurigical problems coupled with the required RF impedance match.

6) Elimination of magnetic assymetries through refinement of assembly procedures.

7) Trial use of samarium-cobalt magnet material which required improved magnet treatment capabilities.

IV. TUBE PERFORMANCE

Focusing Performance - Pulsed and DC Beam

Severe beam transmission problems occurred on Tubes S/N 1, S/N 2, and S/N 3. Only pulsed testing could be carried out on these tubes. Typical beam transmission without RF applied to the tube was in the range of 65 to 85% transmission at 50 mA to the collector. It was difficult to determine precisely where the beam current was striking the helix. All indications based upon previous experience indicated that the beam was intercepted at the beginning of the helix and that the electron beam entrance conditions were incorrect. This could be crudely verified by operating the tube at larger duty cycles where appreciable power dissipation was generated on the helix. The increase in temperature of the magnets around the entrance of the helix indicated that this was the major point of helix current interception.

It was originally thought that some beam convergence could be obtained magnetically by properly adjusting the magnetic field conditions at the entrance to the helix. Under the entrance conditions that existed, this was never possible. After testing Tube No. 3 it was decided that the gun should be redesigned for a smaller beam diameter at the helix entrance. A series of tests were carried out in the beam testing bell jar where a systematic series of spacing variations between various elements of the gun were tried. The attempt was made to choose a combination of dimensions that would maximize the distance from the anode to the minimum diameter location of the beam. This, of course, had to be consistent with the required beam diameter. The gun perveance was maintained at approximately 0.19×10^{-6} in these tests.

The optimum design was chosen and this gun was built into a beam tester (S/N 4) which was a duplicate of a tube except that there were no RF connections to the helix. The helix rods were attenuated over their entire length so that no RF interaction was possible. This allowed the tube to be built without coaxial lines. An assessment could then be made of any magnetic asymmetries which would be due to the gap in the magnet of the cell in which the coax line entered. It also would allow the assessment of the effect of various values of thickness of the magnetic cells in the entrance section. It can be seen in Fig. 10 that the first and second cell at the

beginning of the helix and the last two cells at the end of the helix are not the standard thickness magnets. This tube exhibited 95.9% beam transmission to the collector under dc conditions. This was accomplished at 49.5 mA to the collector with 2000 V on the helix. A series of tests showed that magnetic asymmetries caused by the coaxial line opening in the magnet were not important to focusing. Tests made with different values of cell thickness in the first two cells showed that the thickness value was not critical. Several experimental changes were made in the electron gun by varying the cathode location. As the cathode was pulled back and the perveance became lower, lower beam transmission resulted.

Tube S/N 5 was built. This tube had radial tolerances tightened on the electron gun and cathode assemblies. The prebrazing fit of the entrance region polepieces to the alignment tubing in the input polepiece assembly was made as tight as possible to eliminate any transverse magnetic field components. The gun perveance was set to 0.194×10^{-6}. This tube exhibited 96% transmission at a helix voltage of 2250 V with 51 mA cathode current and 49 mA to the collector. This was the design value of the helix voltage. Dc transmission deteriorated rapidly below this helix voltage, and at 2100 volts could not be operated under dc conditions without excessive helix current. Unfortunately, the helix voltage for RF performance was 2100 volts. As a result, the tube could not be operated CW at 50 mA. Figure 13 shows measured dc beam transmission as a function of cathode current. The helix voltage was fixed at 2250 volts. The anode voltage was varied to vary the cathode current. Anode voltage equals helix voltage at a cathode current of 20 mA. For all higher values of current the anode voltage was greater than 2250 volts.

Conclusions of Focusing

A large part of the experimental effort was spent in working on the focusing problem of this tube in an attempt to understand the cause of the difficulty. Systematic studies of the magnetic field values in the entrance cells of the magnet stack were carried out on each tube. It was determined that most of the intercepted current was being lost at the entrance of the helix. It was determined that magnetic asymmetries were not causing the interception and that the different thickness of the entrance magnet cells did not effect the current interception.

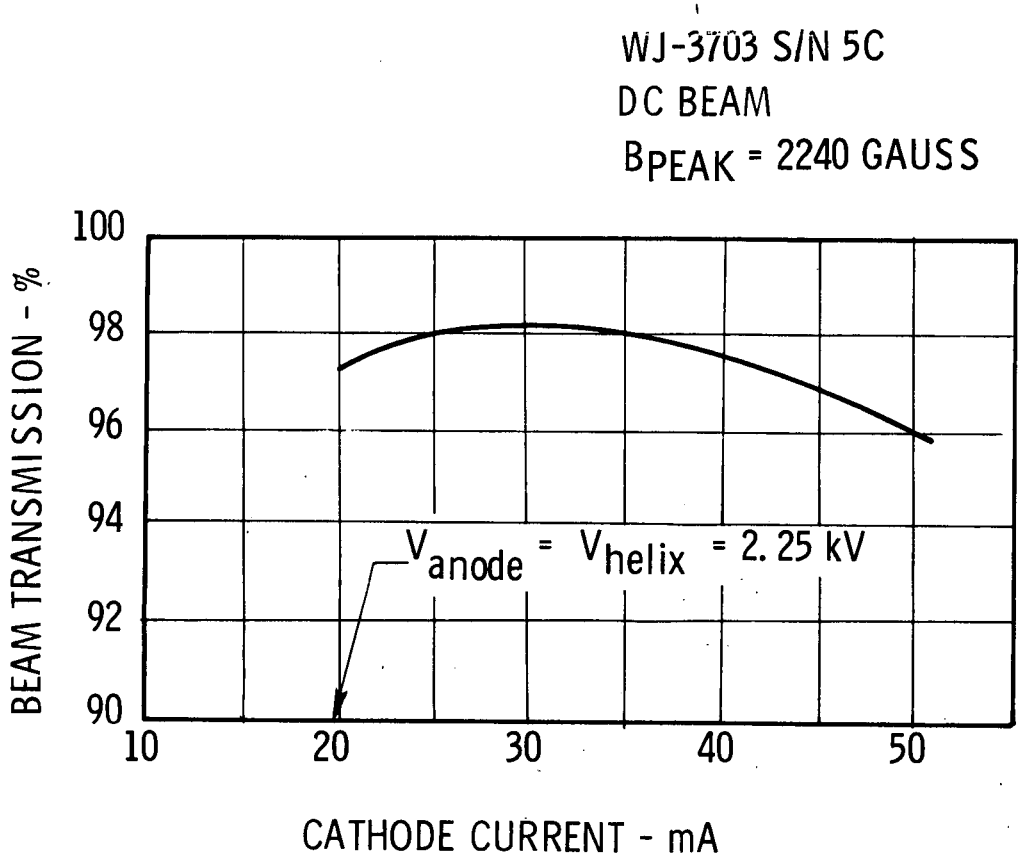

Fig. 13 - Focusing characteristics of S/N 5 as anode voltage was varied with helix voltage at 2250 volts. Above 20 mA, anode voltage was greater than helix voltage.

The design peak magnetic field is 1940 gauss. Focusing tests have been made with this value of cell field throughout the stack. In addition, tests have usually been repeated at 2240 gauss peak. In general, the focusing has been slightly better with the higher field.

Figure 14 shows an analysis of data taken of tubes S/N 4 and S/N 5. S/N 4 was the beam tester. S/N 5 and S/N 5C represent the same tube with different cathode positions in the gun with respect to the focus electrode. The most complete data was taken on S/N 5B. This tube had the lowest gun perveance. The data were taken at fixed values of helix voltage and variable beam current, but have been replotted to show perveance as the variable and beam current as the parameter.

The data for S/N 5B shows that the percent beam transmission improves as the beam perveance is decreased. The unexpected result is that all of the current curves do not fall on the same line. This probably comes about because of the way that the data were taken. The magnet entrance cells were optimized for best beam transmission at 50 mA with the anode/helix lens strength associated with this anode voltage. At the lower currents, the magnetic lenses at the magnet stack entrance were non-optimum which gave slightly lower percent transmission.

The data for S/N 5C were not as extensive, so the lines were drawn in parallel to those for 5B through the existing data points. This shows that the slightly higher perveance gun of S/N 5C gave better beam transmission than S/N 5B.

Only one equivalent point for S/N 4B was taken and it shows even better percent transmission for a given beam perveance. The table in Fig. 14 shows that the lower perveance guns give poorer dc focusing performance. This is the result of the strong electrostatic lens which is formed between helix and anode. At 49.5 mA beam current, the 0.164×10^{-6} perveance gun requires 4510 volts on the anode while at the same current the 0.23×10^{-6} perveance gun requires only 3580 volts on the anode. This results in a 930 volt reduction in the voltage difference across the lens. This strong lens has made adjustment of the entrance conditions of the beam into the helix very difficult. It must be compensated by the magnetic lenses of the first two or three cells of the magnet stack. Elimination of this strong electrostatic lens force, which tends to start the beam so that large scalloping occurs, will undoubtedly give further improvement to the percent beam transmission obtainable as indicated in Fig. 14.

WJ-3703 S/N 5
DC Beam
B_{peak} = 2240 Gauss

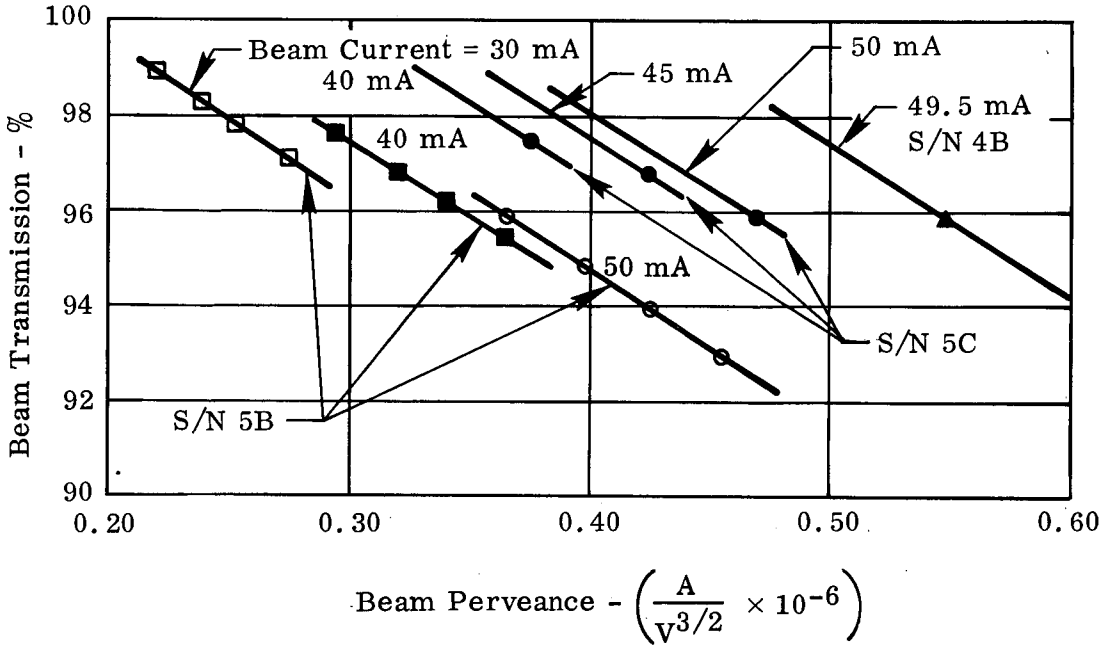

S/N	Gun Perveance
4B	0.23×10^{-6}
5C	0.182×10^{-6}
5B	0.164×10^{-6}

Fig. 14 - Beam transmission tests on S/N 4 and S/N 5. In S/N 5B the cathode was pulled back into the focus electrode by 0.002 inches compared to S/N 5C.

aa25727

Corrective action to give good focusing performance on subsequent tubes should be two-fold. First the gun should be redesigned to bring the gun perveance up to a value just smaller than the beam perveance. This will eliminate the lens problem but will still keep the anode voltage above helix voltage so that ions are blocked from the gun and cathode region. The helix phase velocity should be adjusted so that the beam perveance value at the final set of operating conditions gives a dc beam transmission of 98 percent or greater and a total helix interception under saturated RF power output conditions of not more than 5.0 mA.

Ultimately it may be necessary to raise the peak magnetic field value, which is possible by using samarium cobalt magnets in the entire magnet stack, in order to decrease the final beam diameter. This is not likely to be a requirement, however, because the focusing analysis so far indicates that the low perveance electron gun is causing the major difficulty.

At the same time that the gun is redesigned, the cathode area should be decreased to bring the cathode current density up to 0.50 amp/cm^2. This will lower the area convergence and tend to give a less "thermal" beam. This means that the transverse thermal velocities of the electrons at the beam minimum will be less and the beam cross-sectional current density will be closer to the ideal rectangular shape. This also should reduce beam current interception.

RF Performance

The most significant data for evaluating a tube in the early performance stages is a plot of three basic sets of curves: RF power output, saturation gain, and beam efficiency vs. helix voltage with beam current as the parameter. With experience, these curves can be used to interpret the performance of the tube and give information for evaluating the effects of helix length and helix phase velocity changes.

The goals of the first few tubes built were 25 to 30 watts power output, 37 dB saturation gain, and 28 percent beam efficiency at an operating helix voltage of 2250 volts and 50 mA beam current.

RF performance was evaluated from tubes S/N 1, S/N 3 and S/N 5. S/N 2 had an unrepairable broken connection from helix to the output coax and S/N 4 was a beam tester which was not intended for RF operation.

In the following data taken on the various tubes, the beam current is defined as the current transmitted to the collector under no drive conditions, and beam efficiency was calculated on this basis. This was done because of the large intercepted current at the beginning of the helix. This transmitted current has a large effective diameter which results in additional helix current interception under large signal conditions. However, it is the best approximation at this point to the actual beam current contributing to RF power output.

WJ-3703 S/N 1

The performance of S/N 1 is shown in Fig. 15. This tube was hampered by beam focusing limitations and was tested only under pulse conditions. It operated in the right general range of parameters. The beam current could only be brought up to 40 mA and a further increase in cathode current resulted only in a higher helix interception at the input end and gave no further increase in collector current. The maximum power output reached was 17 watts and the beam efficiency was 20%. Saturation gain exhibited at the maximum efficiency point was 34 dB. Variations of the beam efficiency vs helix voltage and beam current did not follow the normal pattern. This was due primarily to beam focusing problems. This tube was built with a 4-rod helix support. Beam de-focusing under RF drive saturation conditions was serious. This would be expected from a badly scalloping beam which was just clearing the inside of the helix. This tube did establish that performance was in the right general range of power and efficiency.

S/N 3

Figure 16 shows the basic performance curves of S/N 3. This tube showed better performance and allowed 50 mA of beam current to be reached. The general pattern of these curves is what would be more normally expected. The power output reached was 22 watts, the saturation gain was 38 dB, and the beam efficiency reached 23 percent at 50 mA and 1920 volts. This helix voltage was low, indicating that the phase velocity was lower than expected. This is the first 3-rod helix which could be checked for RF performance. RF de-focusing was also serious.

Fig. 17 shows a comparison between measured and computer calculated small signal gain performance vs helix voltage. The close agreement between these curves would lead one to believe that reasonably good modeling of the tube parameters had been done.

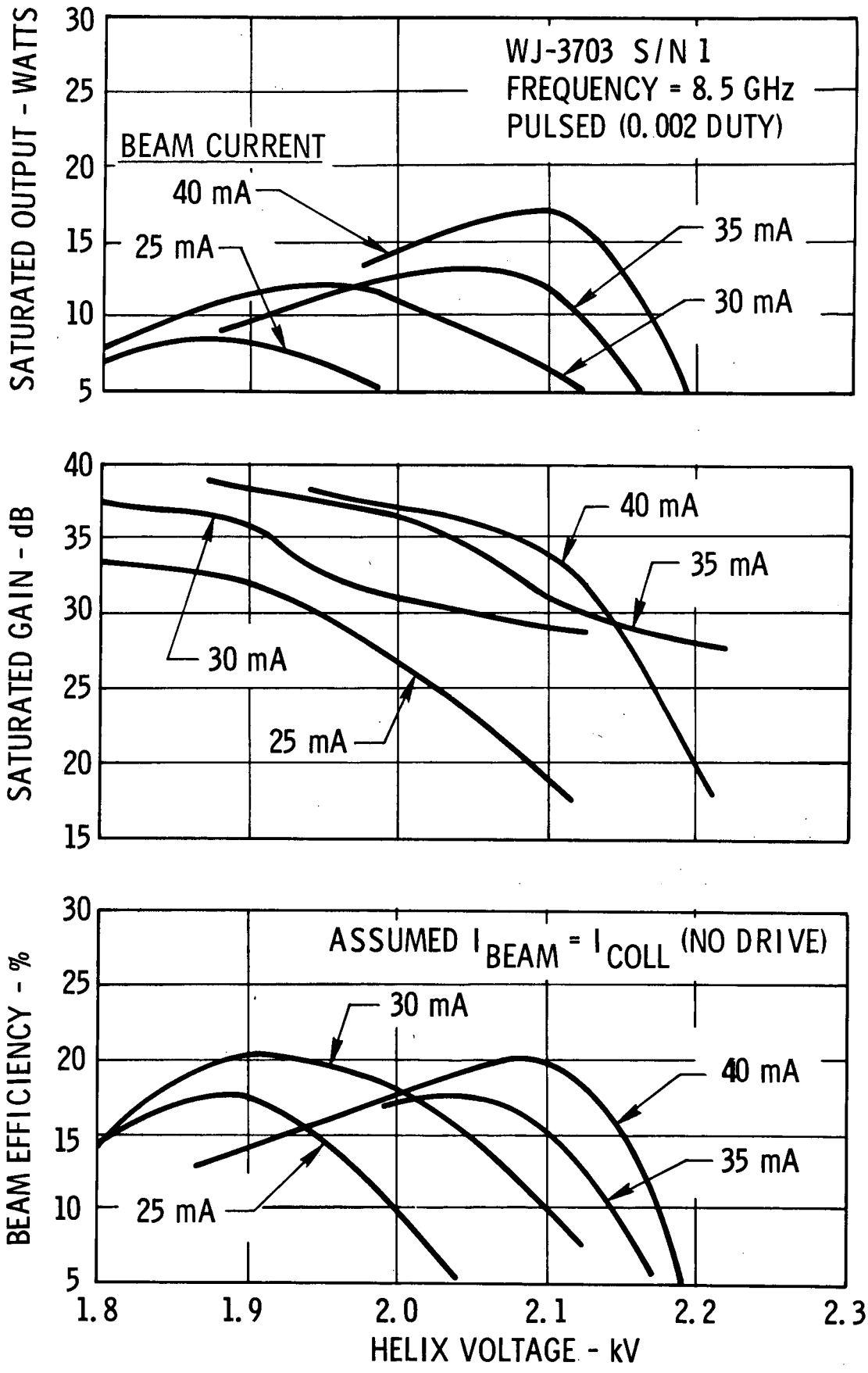

Fig. 15 - Characteristic curves of tube S/N 1.

aa25734

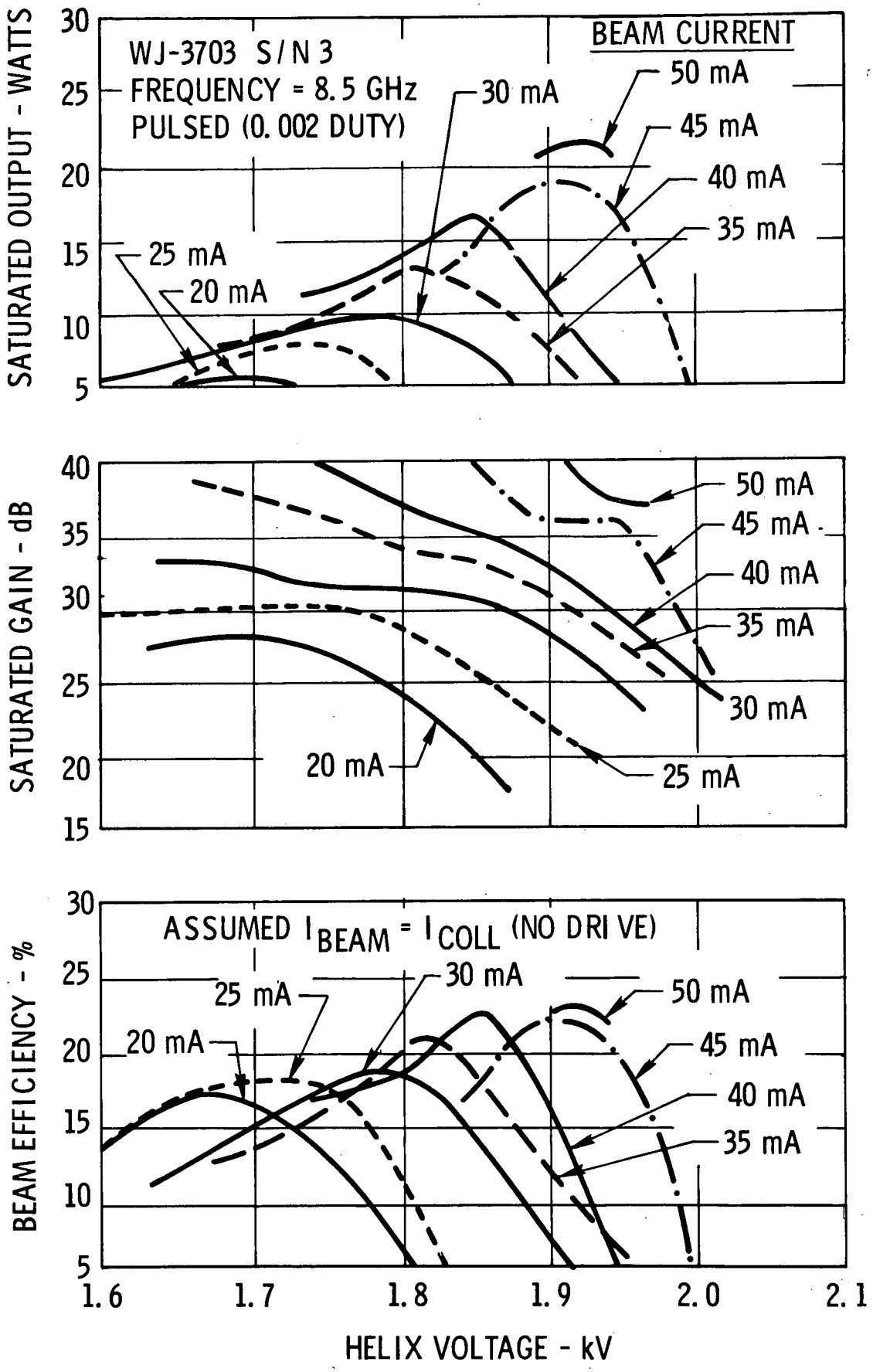

Fig. 16 - Characteristic curves of tube S/N 3.

aa25733

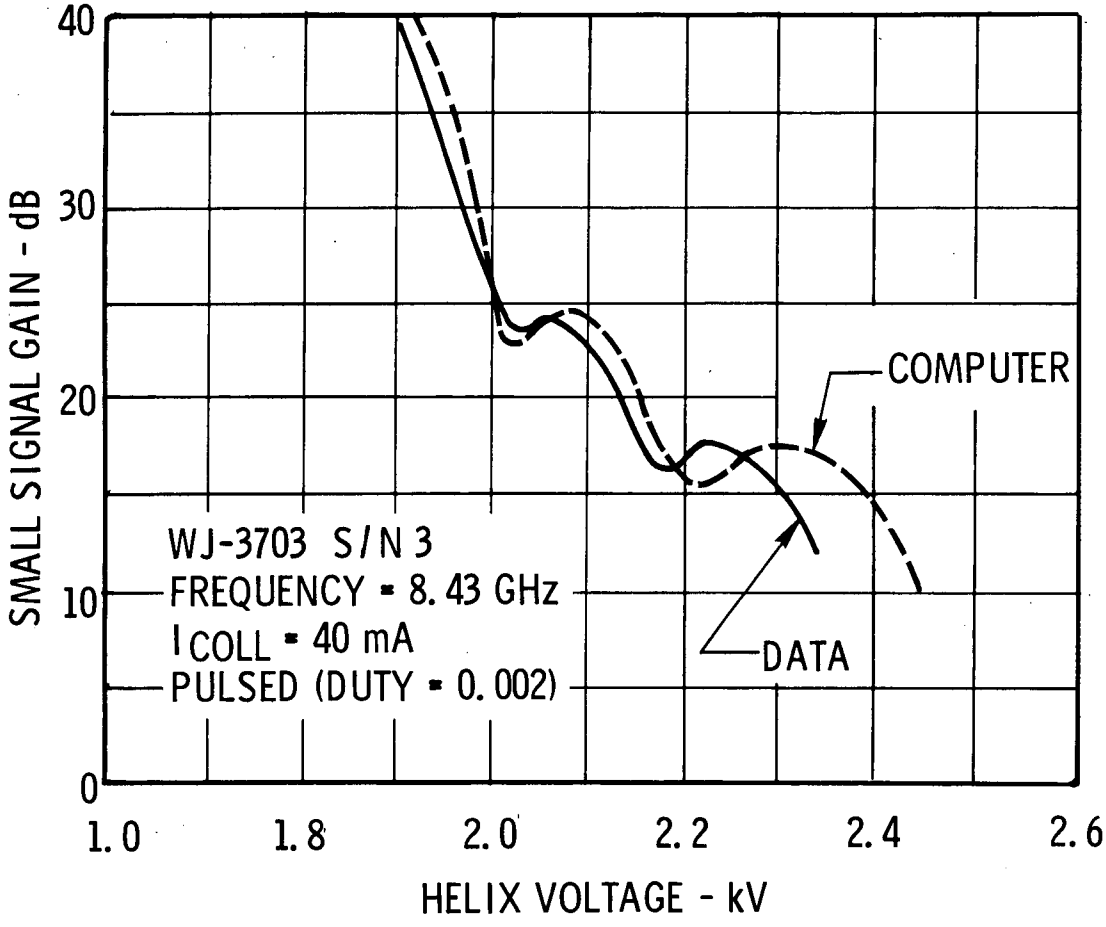

Fig. 17 - Comparison of measured and calculated small signal gain curves. The calculation is based on the actual tube dimensions, lengths, multi-section helix velocities, voltages and current.

S/N 5

An arbitrary limit of 2.0 mA of helix current was set under CW conditions. This limited the helix dissipation to a maximum of 4.5 watts, which was concentrated on the first few turns of the helix. This limit was chosen as the maximum until such time that sufficient experience was obtained to indicate that a higher dissipation level could be safely tolerated without overheating or causing mechanical distortion of the helix. The actual dissipation per unit length of the helix is the important factor. This is not easily evaluated and requires operation of many tubes under CW operating conditions to establish a safe value.

This tube had a redesigned gun which gave improved focusing but which still did not allow CW operation under RF conditions. Helix phase velocity had been increased to raise the operating voltage, but the measured data show that this was not carried far enough. Pole piece and mechanical tolerances on this tube had been tightened to minimize transverse magnetic field components due to loosely fitting polepieces at the helix entrance.

Fig. 18 shows RF measurements made under pulse conditions. These were carried out up to a beam current of 40 mA. At the 40 mA conditions, the power output reached was 17 watts, the saturation gain was 32 dB and the beam efficiency was 22%.

Since there is usually some discrepancy between pulsed and CW measurements, an attempt was made to test this tube under pulsed conditions which simulated dc focusing conditions as closely as possible. The reason that differences are often observed between CW and pulsed tests is that some positive ions are present in the electron beam under CW conditions which contribute ion focusing effects. In order to simulate the CW ion beam that would be present, the tube was operated with dc beam current of approximately 30 mA. This could be done with only 0.6 mA helix current which is 98% beam transmission. At this current the anode voltage was greater than that of the helix. Thus, ions were blocked from draining into the cathode. The collector voltage was slightly depressed below helix to drain ions into the collector and a typical population of ions existed in the dc beam.

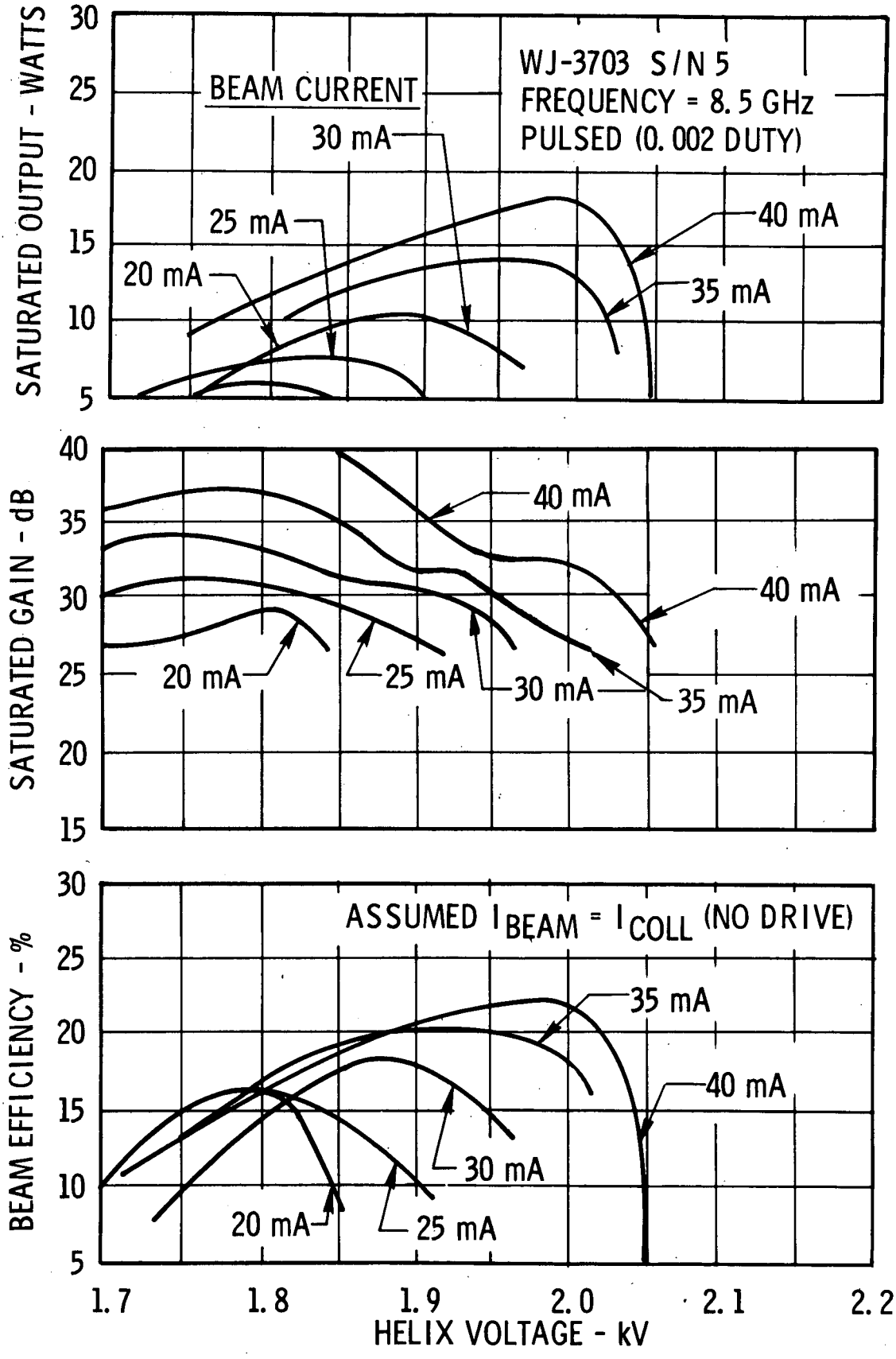

Fig. 18 - Characteristic curves of S/N 5 under pulsed operating conditions.

aa25732

With the tube operating under these conditions on a dc basis, the anode voltage was pulsed positive to get higher values of beam current which were between 40 mA and 58 mA. Fig. 19 shows the characteristics measured under these conditions. If Figs. 18 and 19 are compared at the 40 mA level, it will be seen that the maximum power output and efficiency values occur at the same helix voltage. The partial dc beam data of Fig. 19 has a slightly lower power output and slightly lower beam efficiency as well as a saturation gain which is about 5 dB lower than the pulsed case. This indicates that the ion focusing effect has caused the beam to shrink slightly. The rest of the curves at higher beam currents indicate that power output to 25 watts can be obtained. Maximum beam efficiency still remains at about 22%. The helix voltage at 50 mA of beam current has increased to 2080 volts at its peak efficiency point. The increase at this voltage has been achieved by an increase of the phase velocity of the helix used in S/N 5. The phase velocity increase, however, was not enough to move the operating voltage up to 2250 volts. If the phase velocity had been increased enough to reach this voltage, the tube could have been operated under CW conditions.

Two-Stage Collector Tests

Significant results on the 2-stage collector performance could only be obtained on S/N 3. For some undetermined reason, the beam did not enter properly into the collector of S/N 5 and depressed collector operation on that tube was meaningless.

Fig. 20 shows a plot of efficiency improvement factor of the collector vs collector voltage. This factor is based upon the ratio of power dissipation on the helix and collector under RF drive, with collector at helix voltage, to the power dissipation on these elements as the collector voltage is depressed.

With the 1st and 2nd stages of the collector tied together and operated at the same voltage, the equivalent performance of a 1-stage collector is obtained. It is seen that the efficiency improvement factor maximizes at 1000 volts and reaches a value of 1.52.

With the 1st stage operated at 1100 volts, the 2nd stage can then be operated at lower voltages and a further increase in efficiency improvement factor is realized. It reaches a maximum of 1.73 at 500 volts on the 2nd stage.

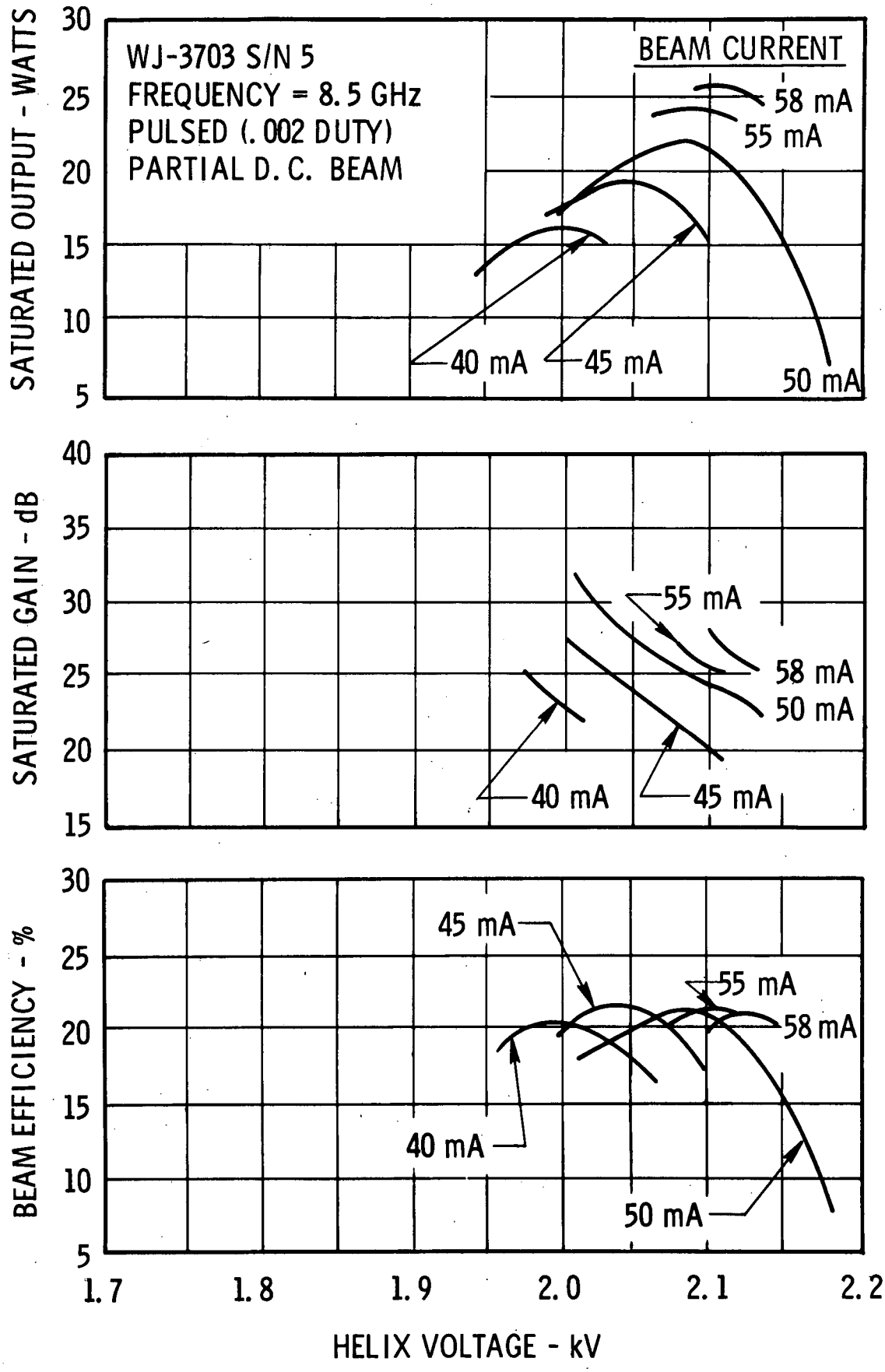

Fig. 19 - Characteristic curves of S/N 5 with a 30 mA dc beam and the anode pulsed to give peak current indicated.

aa25741

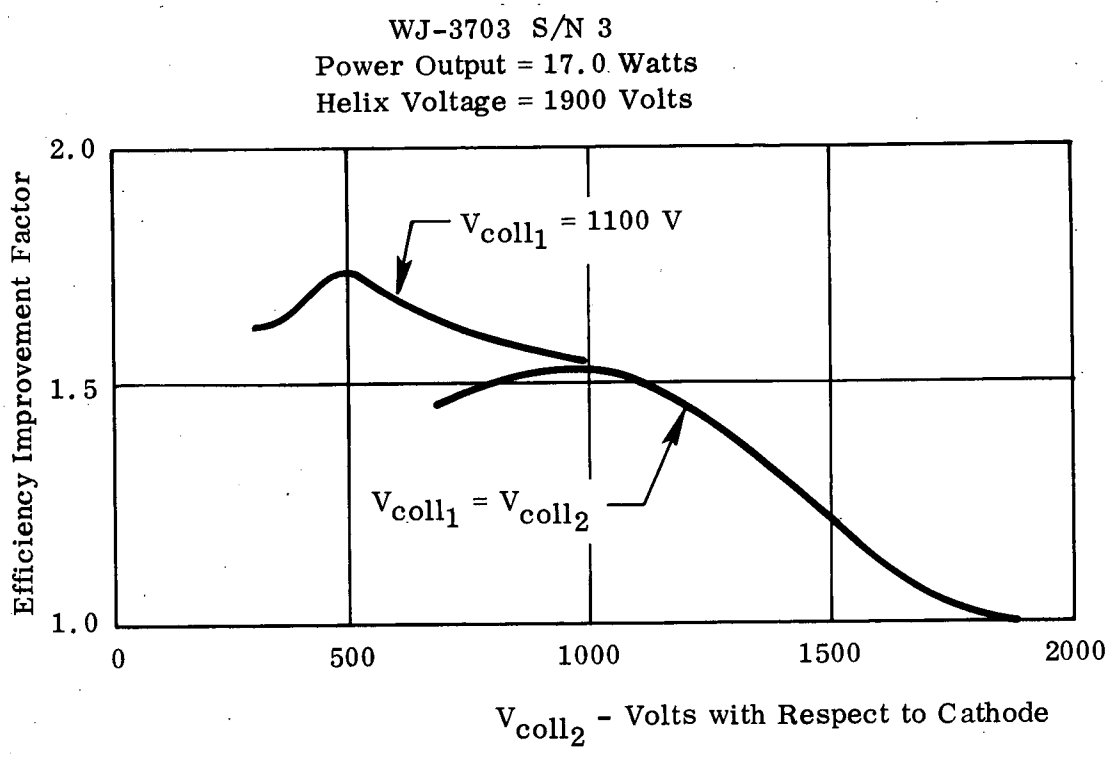

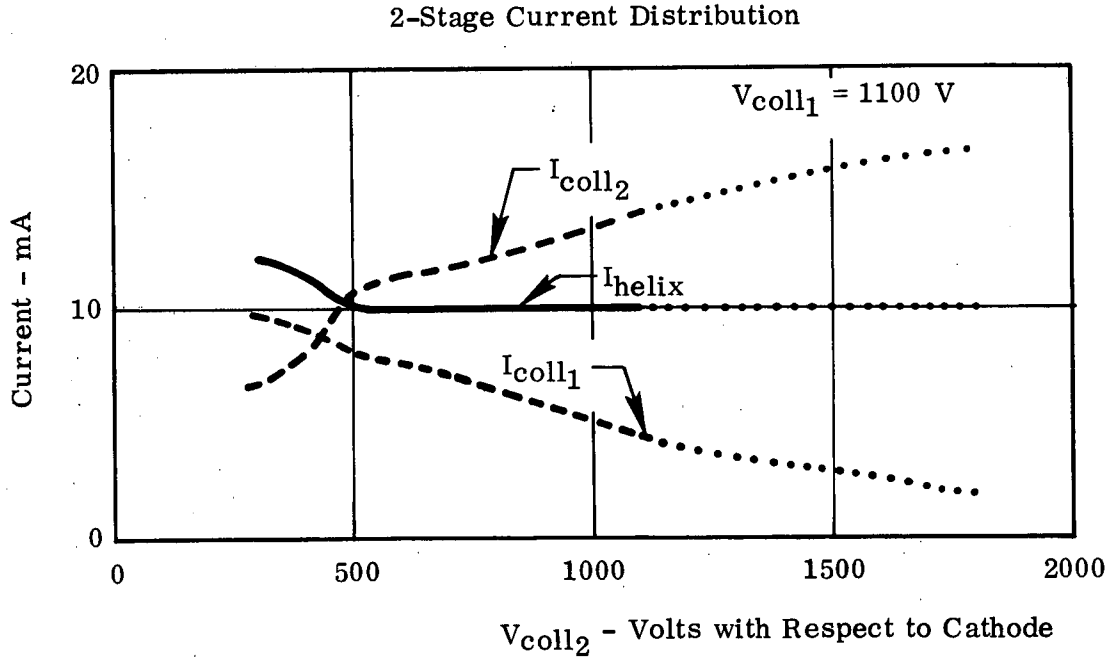

Fig. 20 - Efficiency improvement factor and collector element current distribution versus collector voltage for collector operated as 1- and 2-stage device.

aa25728

To show that the collector is performing as a true 2-stage collector, the current distribution to the helix and collector stages is also plotted in Fig. 20. As the 2nd-stage voltage is lowered, the internal current distribution of the collector changes. The helix current remains constant, however, showing that the helix current is only due to current interception as the beam is passing through the helix on the way to the collector. Down to 500 volts on the 2nd stage, no current is reflected out of the collector onto the helix. At this voltage, helix current begins to increase showing that current is now being reflected out of the collector and is intercepted on the helix. At this point also, the efficiency improvement factor begins to decrease showing that the increased helix dissipation is the contributing cause of rapidly increasing total dissipation. The current distribution with the 2nd-stage collector voltage greater than 1100 volts was not recorded. The estimated current distribution in this region is shown dotted. It is certain that the helix current remained constant as shown.

The conclusion that can be drawn from Fig. 20 is that the 2-stage collector is working and that efficiency improvement beyond that of a 1-stage collector is a reality. The actual efficiency improvement factors that can be achieved will not be known until good focusing under dc and RF operating conditions is achieved. Measurements on similar collector designs on other tube types have shown similar results. One tube with a beam efficiency of 18 percent was able to realize an efficiency improvement factor of 2.5.

Evaluation of RF Tests

RF results are very encouraging at this point in the development. Comparison to the previous successful high efficiency S-band development programs at the 25 watt and 100 watt level shows that after construction of 5 tubes, similar results had been achieved. Mechanical and assembly problems have been overcome and it is believed that the focusing problems are understood. A series of tubes with engineering design changes based upon measurements of each preceding tube can now bring the performance into the required values.

Power output requirements have been reached and with modifications of helix length, pitch, and dielectric loading factor, a CW beam efficiency of 25 to 29% can be achieved. This will depend upon the actual value of beam perveance which can be well focused. Helix phase velocity can be raised if necessary by simply reducing the dielectric loading factor of the helix by using smaller diameter helix support rods while keeping the diameter across the rod to the flat constant.

Saturation gain is easily adjusted to any required value once the power output, gain and efficiency values of the output helix are set. This is accomplished by designing the input helix to provide the balance of gain not supplied by the output helix. This can be accomplished without any effect on power output or efficiency.

CW beam operation could have been achieved on S/N 5 if the helix phase velocity had been high enough to place the operating helix voltage at the design value of 2250 volts where dc focusing was being achieved.

V. PRESENT STAGE OF TUBE DEVELOPMENT

Tube development is now at the point where a relatively small amount of effort will show RF performance at or near design values.

Gun redesign to the higher perveance of about 0.4×10^{-6} is the next step. This will be the first step towards correcting the focusing problems. The ability to operate under CW conditions is a very probable immediate result. Following this, a series of tubes should be built with helix pitch and helix length changes. A sequential series of design, building, testing and redesigning based upon the previous test should be carried out. The tube can be brought to the point of delivering the desired power output, beam efficiency and saturation gain.

At the same time that this helix evaluation is being made, depressed collector operation can be evaluated and optimized. When good RF focusing has been realized, beam entrance conditions into the collector can then be optimized through adjustment of the magnetic lenses at the helix output and the size and position of the collector entrance. Since a two-stage collector can always be operated as a one-stage collector, one- and two-stage collector performance can be evaluated. The completion of the sequence of tubes to evaluate helix design changes should also allow complete evaluation of the two-stage collector. The completion of this series should see the overall efficiency design values being achieved.

Encapsulation of the tube will be a straightforward follow-on step. The same tube envelope support system and cooling schemes will be used which have already been proven in the S-band 100 W tube series. Capsule construction is a direct adaptation of that used in the S-band 100 W tube. Based upon that experience, tubes will be able to meet all environmental conditions.

VI. CONCLUSIONS AND RECOMMENDATIONS

Much has been accomplished on this development program where the original negotiated funds were cut almost in half because of NASA budget cut-backs. This occurred after the program had been under way for approximately three months. Most of the difficult problems have been overcome and electrical results in terms of power level have been achieved, although only under pulsed conditions. Efficiency and gain performance is within reach through construction and testing of several more experimental tube models. It is recommended that the next step in the development of the tube should be a redesign of the electron gun. This should be followed by construction of a series of perhaps eight tubes, to realize the intermediate goal of demonstrating high efficiency at the 25 watt level in a single level tube. This tube should meet all of the power output, gain, efficiency and environmental requirements.

In addition, to realize the original goal of a 25/50 watt dual mode tube will require construction of an additional five to eight experimental tubes following the successful development of the 25 watt single level tube.

REFERENCES

1. Roberts, L.A., "The Efficiency Improvement Program for WJ-274 Traveling-Wave Tube," Final Report, Contract No. NAS1-5923 with NASA Langley Research Center, Watkins-Johnson Company, January 1968.

2. Roberts, L.A., "A 50 Percent Efficient, 100 Watt S-band Traveling-Wave Tube," Final Report, Contract No. 951299 with the Jet Propulsion Laboratory, Watkins-Johnson Company, July 1968.

3. Maurer, D.W. and Pleass, C.M., "The CPC: A Medium Current Density High Reliability Cathode," Bell System Technical Journal, Vol XLVI, No. 10, Dec. 1967.

4. Pierce, J.R., Traveling-Wave Tubes, D. Van Nostrand Co., 1950.